

**Lecture notes for**  
**The Quantum Hall Effect and Beyond:**  
**Topological Insulators**

W. Zhu<sup>1</sup>

<sup>1</sup>*Westlake Institute of Advanced Study,  
Westlake University, Hangzhou, P. R. China\**

**Contents**

<b>The Su-Schrieffer-Heeger (SSH) model</b>	5
<b>Chern Insulator on a lattice</b>	10
Hofstadter Model	11
Hamiltonian and Lattice Translations	11
Hall conductance	13
Haldane Honeycomb Model	14
Graphene (without $t_2$ )	16
Symmetries	17
Chern number	17
<b>Two-dimensional Time-Reversal Topological Insulators</b>	24
Time Reversal Symmetry	24
Spinless particle	24
Spinful particle	26
Kane-Mele Model and Quantum Spin Hall Effect	28
Symmetries	30
1. Time-Reversal symmetry with $t_1$ term	31
2. Inversion symmetry with $t_1$ term	32
3. Symmetries with flux terms	33
$Z_2$ invariant	35

The bulkboundary correspondence: $Z_2$ invariant from the bulk	36
$Z_2$ Invariant as Zeros of the Pfaffian	38
The $Z_2$ invariant for systems with inversion symmetry	41
Comparison with IQHE	43
3D topological insulators	44
<b>Topological Semimetal</b>	45
Nonsymmorphic symmetries enforced band crossings	45
A toy model	46
A spinless model in one-dimension	47
A spinful model in one-dimension	47
Weyl Semimetal	49
<b>Topological Superconductor</b>	52
Majorana edge modes	53
<b>The Kitaev Chain</b>	55
<b>At a glance: periodic table</b>	57
<b>References</b>	59

[3]Reporting of typos, inaccuracies and errors to zhuwei@westlake.edu.cn would be greatly appreciated.

In this part, we will leave the continuue model and go to the lattice tight-binding model. We will introduce the quantum-Hall-like physics on these lattice model and peek into their topological properties.

The geometric phase is a critical concept in the modern theory of crystalline systems. Here we introduce the basic ideas that will enable us to apply the generic Berry phase formalism to band theory. Let us start by discussing the formula for Berry connection and curvature for Bloch states. The electronic properties of the crystal are described within the independent particle approximation by the single-particle Hamiltonian  $H = -\frac{\nabla^2}{2m} + V(r)$  where  $m$  is the electron mass and  $V(r) = V(r + a)$  is a periodic potential. In the Brillouin zone (BZ), the eigenfunction takes the form of  $\psi_{n,\mathbf{q}}(r) = e^{i\mathbf{q}\cdot\mathbf{r}}u_{n,\mathbf{q}}(\mathbf{r})$ , according to the Bloch's theorem. We perform a unitary transformation and introduce the cell-periodic function  $u_{n,\mathbf{q}}(r) = e^{-i\mathbf{q}\cdot r}\psi_{n,\mathbf{q}}(\mathbf{r})$  and  $u_{n,\mathbf{q}}(r) = u_{n,\mathbf{q}}(r + a)$ . Its relevance becomes evident if we take the Schrodinger equation for the Bloch state

$$\left[-\frac{\nabla^2}{2m} + V(r)\right]\psi_{n,\mathbf{q}} = E_{n,\mathbf{q}}\psi_{n,\mathbf{q}} \quad (1)$$

$$\rightarrow H(\mathbf{q})u_{n,\mathbf{q}} = \left[-\frac{(\nabla + i\mathbf{q})^2}{2m} + V(r)\right]u_{n,\mathbf{q}}(r) = E_{n,\mathbf{q}}u_{n,\mathbf{q}}(r) \quad (2)$$

Please note that, the differential equation for  $\psi_{n,\mathbf{q}}$ , a simultaneous eigenfunction of the translation operator and the Hamiltonian, doesnot depend on the wave vector, since  $\mathbf{q}$  only labels the eigenvalues of the translational operator. In contrast,  $\mathbf{q}$  appears as a parameter in ‘‘Hamiltonian’’  $H(\mathbf{q})$ . That is,  $\mathbf{q}$  is just a ‘‘label’’ (good quantum number) in this differential equation. Next,  $\mathbf{q}$  appears as a parameter in calculating Berry curvature and Berry connection, based on the periodic part of wave function  $u_{n,\mathbf{q}}$ .

At this point, we can make the connection with the general Berry phase formalism. We have a parameter dependent Hamiltonian,  $H(R) \rightarrow H(q)$ , and a single Hilbert space  $\mathcal{H}$ , so that for each value of the parameter  $R \rightarrow q$  the set  $|n; R\rangle \rightarrow u_{n,q}$  represents an orthonormal basis for  $\mathcal{H}$ . The parameter space is the Brillouin zone,  $M \rightarrow BZ$ . A slow cyclic variation of  $q$  in the BZ, which may be caused by an external field that enters the Schrodinger equation as a time-dependent variation of the wave vector,  $q \rightarrow q + q(t)$ , will result in the wave function acquiring a geometric phase. To account for these effects, we introduce the Berry

connection and the corresponding Berry curvature vector

$$\mathbf{A}^n(\mathbf{k}) = i\langle u_n(\mathbf{k}) | \nabla_{\mathbf{k}} | u_n(\mathbf{k}) \rangle \quad (3)$$

$$\mathbf{B}^n(\mathbf{k}) = \nabla \times \mathbf{A}^n(\mathbf{k}) = \partial_y A_x - \partial_x A_y = i \left\langle \frac{\partial u_n}{\partial q_x} \middle| \frac{\partial u_n}{\partial q_y} \right\rangle - \left\langle \frac{\partial u_n}{\partial q_y} \middle| \frac{\partial u_n}{\partial q_x} \right\rangle \quad (4)$$

Similarly, the berry phase is defined in integral in the BZ:  $\gamma_n = \int_{C_{BZ}} d\mathbf{q} \cdot i\langle u_n(\mathbf{q}) | \nabla_{\mathbf{q}} | u_n(\mathbf{q}) \rangle$ .

In addition, someone could also see the above connection from the Hall conductance calculations, via the form of the velocity operator :

$$\begin{aligned} \langle n, q | v_\gamma | m, q' \rangle &= \int dr \psi_{n,\mathbf{q}}^* \left[ -\frac{(i\nabla - e\mathbf{A})_\gamma}{m} \right] \psi_{m,\mathbf{q}'} \\ &= \int dr u_{n,\mathbf{q}}^*(r) e^{-i\mathbf{q}\cdot r} \left[ -\frac{(i\nabla - e\mathbf{A})_\gamma}{m} \right] u_{m,\mathbf{q}'}(r) e^{i\mathbf{q}'\cdot r} \\ &= \int dr u_{n,\mathbf{q}}^*(r) \left[ -\frac{(i\nabla + \mathbf{q}' - e\mathbf{A})_\gamma}{m} \right] u_{m,\mathbf{q}'}(r) \\ &= \int dr u_{n,\mathbf{q}}^*(r) \frac{\partial H(\mathbf{q})}{\partial \mathbf{q}} u_{m,\mathbf{q}}(r) \delta(\mathbf{q} - \mathbf{q}') e^{i(\mathbf{q}' - \mathbf{q})\cdot r} \\ &= \langle u_{n,\mathbf{q}} | \frac{\partial H(\mathbf{q})}{\partial \mathbf{q}} | u_{m,\mathbf{q}} \rangle \delta(\mathbf{q} - \mathbf{q}') \end{aligned}$$

Thus the Hall conductance becomes

$$\begin{aligned} \sigma_H &= \frac{\hbar e^2}{V} \text{Im} \left[ \sum_{n,m,q,k} n_F(E_{n,q}) \frac{\langle n, q | v_\alpha | m, k \rangle \langle m, k | v_\beta | n, q \rangle - \langle m, k | v_\alpha | n, q \rangle \langle n, q | v_\beta | m, k \rangle}{(E_{m,k} - E_{n,q})^2} \right] \\ &= \frac{\hbar e^2}{\hbar^2 V} \text{Im} \left[ \sum_{n,m,q,k} n_F(E_{n,q}) \frac{\langle n, q | \frac{\partial \bar{H}}{\partial k_x} | m, k \rangle \langle m, k | \frac{\partial \bar{H}}{\partial k_y} | n, q \rangle - \langle m, k | \frac{\partial \bar{H}}{\partial k_y} | n, q \rangle \langle n, q | \frac{\partial \bar{H}}{\partial k_x} | m, k \rangle}{(E_{m,k} - E_{n,q})^2} \right] \\ &= \frac{\hbar e^2}{\hbar^2 V} \text{Im} \left[ \sum_{E_{n,q} < E_F} \left\langle \frac{\partial n}{\partial k_x} \middle| \frac{\partial n}{\partial k_y} \right\rangle - \left\langle \frac{\partial n}{\partial k_y} \middle| \frac{\partial n}{\partial k_x} \right\rangle \right] \end{aligned} \quad (5)$$

$$\begin{aligned} \sigma_{xy} &= \frac{\hbar e^2}{\hbar^2} \text{Im} \left[ \sum_{E_{n,k} < E_F} \int \frac{d\mathbf{k}}{(2\pi)^2} \left\langle \frac{\partial n}{\partial k_x} \middle| \frac{\partial n}{\partial k_y} \right\rangle - \left\langle \frac{\partial n}{\partial k_y} \middle| \frac{\partial n}{\partial k_x} \right\rangle \right] \\ &= \frac{e^2}{2\pi\hbar} \sum_{E_{n,k} < E_F} C_n \end{aligned} \quad (6)$$

$$C_n = \frac{1}{2\pi} \int_{BZ} d\mathbf{k} \mathbf{B}^n(\mathbf{k}) \quad (7)$$

## THE SU-SCHRIEFFER-HEEGER (SSH) MODEL

The simplest non-trivial topology : 1-d lattice. Peierls instability makes the atoms dimerize, which could occur in Polyacetylene Structure.

Consider only the nearest interaction, we have:

$$\hat{H} = \sum_{n=1}^M \hat{c}_n^\dagger \hat{c}_{n+1} t_n + h.c. \quad (8)$$

Rewrite it in matrix form:  $\hat{H} = \sum_{mn} \hat{c}_m \tilde{H}_{mn} c_n$ , we have

$$\tilde{H}_{mn} = \begin{pmatrix} 0 & t_1 & 0 & \cdots & t_M^* \\ t_1^* & 0 & t_2 & \cdots & 0 \\ 0 & t_2^* & 0 & \cdots & 0 \\ \vdots & \vdots & \vdots & \ddots & \vdots \\ t_M & 0 & 0 & t_{M-1}^* & 0 \end{pmatrix} \quad (9)$$

In the case when  $t = t_n$ ,  $\hat{c}_n$  satisfy the Bloch condition, we can transform it into momentum space, with  $\hat{c}_n = \frac{1}{\sqrt{M}} \sum_k \hat{c}_k e^{ikx_n}$ , we can easily get

$$\hat{H} = \sum_k \hat{c}_k^\dagger \hat{c}_k (t e^{ika} + t^* e^{-ika}) = \sum_k \hat{c}_k^\dagger \hat{c}_k E(k) \quad (10)$$

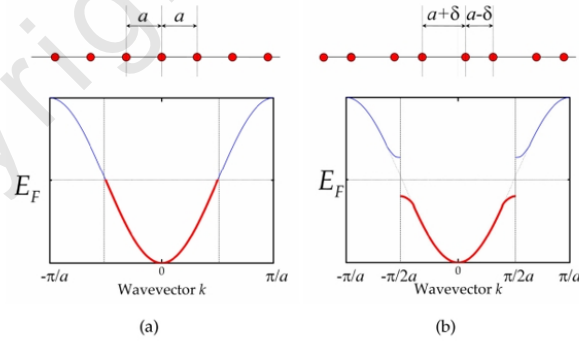


FIG. 1: Schematic plot of 1-d free electron model.

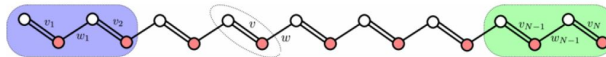


FIG. 2: Polyacetylene Structure.

which gives us the dispersion relation  $E(k) = te^{ika} + t^*e^{-ika} = 2t \cos ka$ .

More generally,  $t_n$  can be different from each other, for example, if they are all different up to 4, but have a super-periodicity with  $t_5 = t_1$ , then there will have 4 sub-bands, in the example we will consider below, we have two  $t$ ,  $t_1 \neq t_2$ , and we have two sub-bands.

If each atom have a valance electron, then the above mentioned energy band structure  $E(k) = 2t \cos ka$  is not the stable fundamental mode, it will dimerizes to lower the total energy, that means we'll get following coupling case with the Hamiltonian:

$$H = \sum_{n=1}^N (v_n c_{n,1}^\dagger c_{n,2} + w_n c_{n,2}^\dagger c_{n+1,1} + h.c.) \quad (11)$$

with  $M = 2N$ .

For a more beautiful notation, define  $\mathbf{c}_n^\dagger = (c_{n,1}^\dagger, c_{n,2}^\dagger) = (c_{2n-1}^\dagger, c_{2n}^\dagger)$ , then we have  $H = \sum_{m,n=1}^N \mathbf{c}_m^\dagger H_{mn} \mathbf{c}_n$  with

$$\mathbf{c}_n^\dagger H_{nn} \mathbf{c}_n = \begin{pmatrix} c_{n,1}^\dagger & c_{n,2}^\dagger \end{pmatrix} \begin{pmatrix} 0 & v_n \\ v_n^* & 0 \end{pmatrix} \begin{pmatrix} c_{n,1} \\ c_{n,2} \end{pmatrix} = \begin{pmatrix} c_{n,1}^\dagger & c_{n,2}^\dagger \end{pmatrix} U_n \begin{pmatrix} c_{n,1} \\ c_{n,2} \end{pmatrix} \quad (12)$$

and

$$\mathbf{c}_n^\dagger H_{n,n+1} \mathbf{c}_{n+1} = \begin{pmatrix} c_{n,1}^\dagger & c_{n,2}^\dagger \end{pmatrix} \begin{pmatrix} 0 & 0 \\ w_n & 0 \end{pmatrix} \begin{pmatrix} c_{n+1,1} \\ c_{n+1,2} \end{pmatrix} = \begin{pmatrix} c_{n,1}^\dagger & c_{n,2}^\dagger \end{pmatrix} T_n \begin{pmatrix} c_{n+1,1} \\ c_{n+1,2} \end{pmatrix} \quad (13)$$

$$\mathbf{c}_{n+1}^\dagger H_{n+1,n} \mathbf{c}_n = \begin{pmatrix} c_{n+1,1}^\dagger & c_{n+1,2}^\dagger \end{pmatrix} T_n^\dagger \begin{pmatrix} c_{n,1} \\ c_{n,2} \end{pmatrix} \quad (14)$$

when  $|m - n| > 1$ , we have  $H_{mn} = 0$ .

So, we have

$$H = \begin{pmatrix} U_1 & T_1 & 0 & \cdots & T_N^\dagger \\ T_1^\dagger & U_2 & T_2 & \cdots & 0 \\ 0 & T_2^\dagger & U_3 & \cdots & 0 \\ \vdots & \vdots & \vdots & \vdots & \vdots \\ T_N & 0 & 0 & \cdots & U_N \end{pmatrix} \quad (15)$$

Using three Pauli matrices  $\sigma_x = \begin{pmatrix} 0 & 1 \\ 1 & 0 \end{pmatrix}$ ,  $\sigma_y = \begin{pmatrix} 0 & -i \\ i & 0 \end{pmatrix}$ ,  $\sigma_z = \begin{pmatrix} 1 & 0 \\ 0 & -1 \end{pmatrix}$ , We get  $U = \text{Re}(v)\sigma_x - \text{Im}(v)\sigma_y$ ,  $T = \frac{1}{2}w(\sigma_x - i\sigma_y)$ .

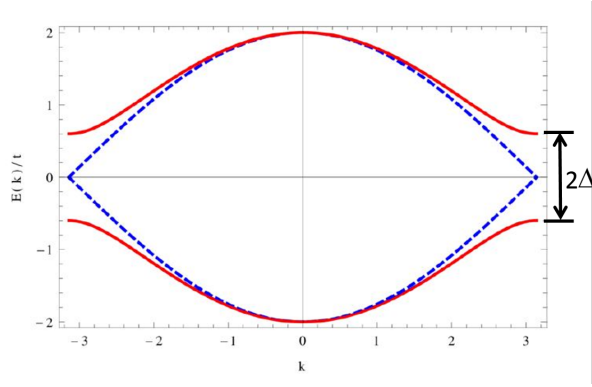


FIG. 3: The energy gap os SSH is  $|v| - |w| = \pm\Delta$ .

Using  $\mathbf{c}_n = e^{ik(n-1)b}\mathbf{c}_1$ , we have

$$\hat{H} = \sum_k \begin{pmatrix} c_{k,1}^\dagger & c_{k,2}^\dagger \end{pmatrix} H(k) \begin{pmatrix} c_{k,1} \\ c_{k,2} \end{pmatrix}, \quad H(k) = \mathbf{h}(k) \cdot \boldsymbol{\sigma} \quad (16)$$

where

$$h_x(k) = \text{Re}(v) + |w| \cos(kb + \arg(w)) \quad (17)$$

$$h_y(k) = -\text{Im}(v) + |w| \sin(kb + \arg(w)) \quad (18)$$

$$h_z(k) = 0 \quad (19)$$

with eigen-energy

$$E(k) = |h(k)| = \pm \sqrt{h_x^2 + h_y^2 + h_z^2} = \pm \sqrt{|v|^2 + |w|^2 + 2|v||w|\cos(kb + \arg(v) + \arg(w))}$$

and eigen-wavefunctions  $|\pm\rangle = \begin{pmatrix} \pm e^{-i\phi(k)} \\ 1 \end{pmatrix}$  with  $\tan\phi = h_y/h_x$  or  $e^{i\phi_k} = \frac{h_x + ih_y}{|h_x + ih_y|}$ .

For example, set  $\arg(v) = \arg(w) = 0$ , we have a gap opening in the band structure, as shown below.

Energy-band description is not completed, it can give us many information, but not the whole, others are hidden in the wave-function. Alternatively, recalling  $H(k) = \mathbf{h}(k) \cdot \boldsymbol{\sigma}$ , the Hamiltonian should contain the whole information, but we have only used  $|h|$ , in topological aspect,  $\mathbf{h}(k)$  will suffices.

Set  $\arg(v) = 0$ ,  $kb = [0, 2\pi]$ , we have two cases  $|w| < |v|$  when **inter** < **intra** and  $|w| > |v|$ , when **inter** > **intra**.

We can define the winding number below, to distinguish these two phases. When we

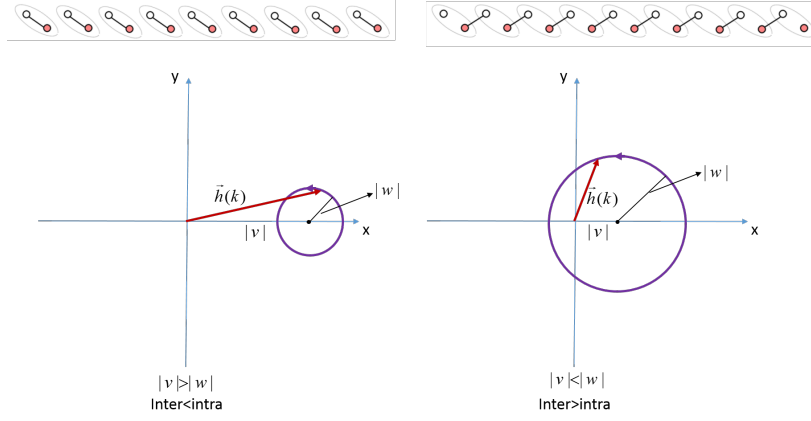


FIG. 4: The winding number of SSH model.

write  $H(k) = \begin{pmatrix} 0 & h^*(k) \\ h(k) & 0 \end{pmatrix}$ , we define  $\ln(h) = \ln(|h|)e^{i \arg(h)} = \ln(|h|) + i \arg(h)$  and Berry connection

$$A_k^- = i \langle - | \frac{d}{dk} | - \rangle = \frac{d\phi_k}{2dk}. \quad (20)$$

Here we need some math here

$$\begin{aligned} d(e^{i\phi_k}) &= e^{i\phi_k} i \frac{d\phi_k}{dk} = \frac{d_k(h_x + ih_y)}{|h_x + ih_y|} - \frac{(h_x + ih_y)d_k(|h_x + ih_y|)}{|h_x + ih_y|^2} \\ &\rightarrow i \frac{d\phi_k}{dk} = \frac{d_k(h_x + ih_y)}{h_x + ih_y} + \frac{d_k(|h_x + ih_y|)}{|h_x + ih_y|} \end{aligned} \quad (21)$$

Thus the berry phase

$$\begin{aligned} \nu &= \frac{1}{2\pi i} \int_{-\pi}^{\pi} dk A_k^- = \frac{1}{2\pi i} \int_{-\pi}^{\pi} dk \frac{d\phi_k}{2dk} = \frac{1}{2\pi i 2} \int_{-\pi}^{\pi} dk \frac{d_k(h_x + ih_y)}{h_x + ih_y} = \frac{1}{2\pi i} \int_{-\pi}^{\pi} dk \frac{d_k(v + we^{ik})}{v + we^{ik}} = \\ &= \frac{1}{2\pi i} \int_{-\pi}^{\pi} \frac{wd(e^{ik})}{v + we^{ik}} = \frac{1}{2\pi i} \oint_{|z|=1} \frac{dz}{\frac{v}{w} + z} \end{aligned} \quad (22)$$

The results are  $|w| > |v|, \nu = 1, \mathbf{inter} > \mathbf{intra}$  and  $|w| < |v|, \nu = 0, \mathbf{inter} < \mathbf{intra}$  (see Fig. 4)

A example, by setting  $N = 20, M = 2N = 40, w = 1, v = 0.5$ , we get eigen-energys and eigen modes in Fig. 5. We see two zero modes in the spectrum, which relate to the edge state in the spatial space.

We have already seen, for  $|w| > |v|$  or  $|w| < |v|$ , we got different winding number, means there is a topological transition at  $|w| = |v|$ . In the energy-band point of view, it means the



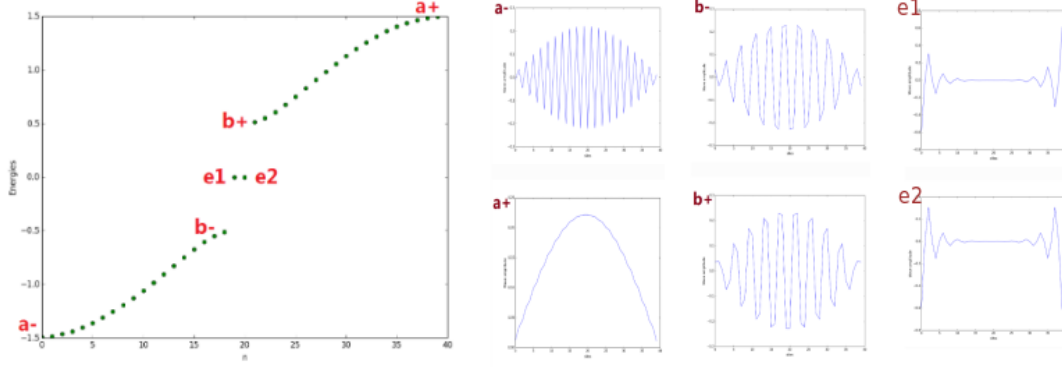


FIG. 5: The edge state of SSH model.

gap between two energy bands closes (across each other) and reopens. There are two ways to change the winding number and get a topological transition: 1. Pull the path through the origin in the  $h_x - h_y$  plane. 2. Lift it out of the plane (breaking the chiral symmetry). In either case, one will find the gap closes at the critical point.

At last, we point out, the SSH model hosts a chiral symmetry if the  $h_z = 0$ :

$$\sigma_z \hat{H} \sigma_z = -\hat{H} \quad (23)$$

The consequence is, for eigenstates  $|\psi_n\rangle$ , we have  $H|\psi_n\rangle = E_n|\psi_n\rangle$ , and then  $H\Sigma_z|\psi_n\rangle = -\Sigma_z H|\psi_n\rangle = -\Sigma_z E_n|\psi_n\rangle = -E_n\Sigma_z|\psi_n\rangle$ . So the energy eigenstates always occur in pair.

## CHERN INSULATOR ON A LATTICE

We present a understanding of the quantum Hall problem from a lattice perspective. We present a detailed exposition of the problem of a 2D lattice pierced by a uniform magnetic field and learn about magnetic translation generators, the magnetic translation group, the Hofstadter problem, the Diophantine equation, explicit gauge fixing, and Hall conductance on the square lattice.

The lattice model with external magnetic field is

$$H = \frac{1}{2m} \int dx \Psi^\dagger(x) [(\mathbf{p} - e\mathbf{A})^2] \Psi(x) \quad (24)$$

where we see that the relevant operator is the ordinary momentum supplemented by the vector field term  $\mathbf{A}$ . The field operators  $\Psi(x) = \sum_\alpha \phi_\alpha(x) c_\alpha$  can be expanded in any one-particle basis set of orbitals labeled by quantum numbers,  $\phi_\alpha(x)$ , and associated destruction operators  $c_\alpha$ . In the rather drastically restricted basis set, setting for a while  $A = 0$ , the Hamiltonian reads:

$$H = \sum_{r,r'} h_{r,r'} c_r^\dagger c_{r'} + h.c. + \sum_r \epsilon_r c_r^\dagger c_r \quad (25)$$

where  $h_{r,r'}$  represents the amplitude for the electron to hop, conserving its spin, from orbital  $i$  to some neighbor  $j$  on the lattice  $h_{r,r'} = \int \phi(r)^* [(\mathbf{p})^2/2m] \phi(r')$ .

How do we treat a magnetic field in a tight-binding scheme? One way is that a reasonable gauge-invariant way of introducing the vector potential is by modifying the hopping amplitudes according to the so-called Peierls' substitution:

$$h_{r,r'} \rightarrow h_{r,r'}^A = h_{r,r'} e^{ie \int_r^{r'} \mathbf{A} \cdot d\mathbf{l}} \quad (26)$$

where the line-integral is calculated on a straight line connecting  $r$  to  $r'$  [We should not simply substitute  $\mathbf{p} \rightarrow \mathbf{p}' = \mathbf{p} + e\mathbf{A}$  in the previous expression for  $h_{r,r'}$ , because it is not gauge invariant]. Such a line-integral suggests that we can introduce an average vector potential living on the link. Note that if you change  $A = A' + \nabla\chi$  then the phase factors change as:  $e^{i \int_r^{r'} \mathbf{A} \cdot d\mathbf{l}} = e^{ie \int_r^{r'} \mathbf{A}' \cdot d\mathbf{l}} e^{i(\chi_r - \chi_{r'})}$ , and you can easily get rid of these extra phase factors by a unitary transformation that changes  $c_r = c_r' e^{i\chi_r}$ .

## Hofstadter Model

### *Hamiltonian and Lattice Translations*

We consider

$$H = \sum_{ij} t e^{i\theta_{i,i+1}^x} c_{ij}^\dagger c_{i+1,j} + h.c. + \sum_{ij} t e^{i\theta_{j,j+1}^y} c_{i,j}^\dagger c_{i,j+1} + h.c. \quad (27)$$

and

$$\theta_{i,i+1}^x = \frac{e}{\hbar} \int_{ij}^{i+1,j} d\mathbf{l} \cdot \mathbf{A}, \quad \theta_{j,j+1}^y = \frac{e}{\hbar} \int_{ij}^{i,j+1} d\mathbf{l} \cdot \mathbf{A} \quad (28)$$

so that we have

$$2\pi\phi_{ij} = \frac{e}{\hbar} \int_{unit} \mathbf{A} \cdot d\mathbf{l} = \theta_{i+1,j}^y - \theta_{i,j}^y - \theta_{i,j+1}^x + \theta_{i,j}^x \quad (29)$$

Next we would like to specify the gauge, we select the Landau gauge  $A_y = Bx = 2\pi\phi i$ , for the special case of rational flux per plaquette,  $\phi = p/q$ , where p, q are relatively prime.

The translational operator doesnot commute in the elementary unit cell, but commute in a enlarged magnetic unit cell. Here we define the tranalational operators as

$$\begin{aligned} T^x &= \sum_{mn} e^{i\theta_{m,m+1}^x} c_{mn}^\dagger c_{m+1,n} = \sum_{mn} c_{mn}^\dagger c_{m+1,n} \\ T^y &= \sum_{mn} e^{i\theta_{n,n+1}^y} c_{mn}^\dagger c_{m,n+1} = \sum_{mn} e^{i2\pi\phi m} c_{mn}^\dagger c_{m,n+1} \end{aligned} \quad (30)$$

Let us prove that  $T^x$  and  $T^y$  doesnot commute (see equations above) and

$$T^x T^y = e^{i2\pi\phi} T^y T^x \quad (31)$$

which leads to

$$(T^x)^q T^y = e^{i2\pi\phi q} T^y (T^x)^q = T^y (T^x)^q \quad (32)$$

We hence have two operators,  $(T^x)^q, T^y$  which commute between themselves and commute with the Hamiltonian.

The action of these two operators on single-particle states is that of translation by one lattice constant in the y-direction and by q lattice constants in the x-direction

$$(T^x)^q |k_x, k_y \rangle = e^{ik_x q a} |k_x, k_y \rangle, \quad T^y |k_x, k_y \rangle = e^{ik_y a} |k_x, k_y \rangle \quad (33)$$

The new translational unit cell in the x-direction is called the magnetic unit cell, and it is q times larger than the usual unit cell, because the unit cell is q times larger in the

x-direction, the magnetic BZ is  $q$  times smaller:  $k_x \in [0, 2\pi/q]$ ,  $k_y \in [0, 2\pi]$ , or  $-\pi < k_x q < \pi$ ,  $-\pi < k_y < \pi$ .

Assume  $|k_x, k_y\rangle$  is an eigenstate of the Hamiltonian. Because  $T^{x,y}$  do not commute between themselves,  $T^x|k_x, k_y\rangle$  cannot be an eigenstate of the Hamiltonian at the same wavevector. Instead,

$$T^y|k_x, k_y\rangle = e^{ik_y a}|k_x, k_y\rangle, T^y(T^x|k_x, k_y\rangle) = e^{-i2\pi\phi}T^y|k_x, k_y\rangle = e^{i(k_y - 2\pi\phi)}|k_x, k_y\rangle \quad (34)$$

The eigenvalue under  $T^y$  of  $T^x|k_x, k_y\rangle$  is  $k_y - 2\pi\phi$ , which leads us to conclude that  $T^x|k_x, k_y\rangle = |k_x, k_y - 2\pi\phi\rangle$ . Thus, there exist  $q$ -fold degeneracy with different  $k_y$  and same  $k_x$ :  $|k_x, k_y\rangle, |k_x, k_y - 2\pi\phi\rangle, \dots, |k_x, k_y - 2\pi\phi(q-1)\rangle$

Next we can construct the wave function as

$$|\Psi\rangle = \frac{1}{q} \sum_{r=1}^q \int_{-\pi}^{\pi} \frac{dk_x}{2\pi} \int_{-\pi/q}^{\pi/q} \frac{dk_y}{2\pi/q} a_r(k_x, k_y) |k_x, k_y\rangle \quad (35)$$

where we define  $a_r(k_x, k_y) = a(k_x, k_y + 2\pi\phi r)$ .

The (discrete) Schrödinger equation now reads

$$\begin{aligned} H|\Psi\rangle &= \left[ \sum_{x,y} |x+1, y\rangle\langle x, y| + |x-1, y\rangle\langle x, y| + e^{i2\pi\phi r} |x, y+1\rangle\langle x, y| + e^{-i2\pi\phi r} |x, y-1\rangle\langle x, y| \right] |\Psi\rangle \\ &= \sum_{x,y} \frac{1}{q} \sum_{r=1}^q \int_{-\pi}^{\pi} \frac{dk_x}{2\pi} \int_{-\pi/q}^{\pi/q} \frac{dk_y}{2\pi/q} a_r(k_x, k_y) \sum_{x,y} e^{ik_x x + ik_y y} [|x+1, y\rangle + |x-1, y\rangle + e^{i2\pi\phi r} |x, y+1\rangle + e^{-i2\pi\phi r} |x, y-1\rangle] \\ &= E|\Psi\rangle = E \frac{1}{q} \sum_{r=1}^q \int_{-\pi}^{\pi} \frac{dk_x}{2\pi} \int_{-\pi/q}^{\pi/q} \frac{dk_y}{2\pi/q} a_r(k_x, k_y) |k_x, k_y\rangle \end{aligned} \quad (36)$$

which leads to

$$a_{r-1}(k_x, k_y) e^{ik_x} + a_{r+1}(k_x, k_y) e^{-ik_x} + a_r(k_x, k_y) e^{i(k_y + 2\pi\phi r)} + a_r(k_x, k_y) e^{-i(k_y - 2\pi\phi r)} = E a_r(k_x, k_y) \quad (37)$$

This equation is also known as the Harper equation and plays an important role in the theory of the electronic structure of incommensurate systems. The amplitudes  $a_r(k_x, k_y)$  are periodic functions on the magnetic Brillouin zone and thus satisfy

$$a_r(k_x + 2\pi, k_y) = a_r(k_x) \quad (38)$$

$$a_r(k_x, k_y + 2\pi\phi) = a_{r+1}(k_x, k_y) \quad (39)$$

$$a_{r+q}(k_x, k_y) = a_r(k_x, k_y) \quad (40)$$

This equation has a set of  $q$  linearly independent solutions  $\Psi^j$  ( $j = 1, \dots, q$ ). Each solution  $\Psi^j$  has an eigenvalue  $E_j(k)$ .

For arbitrary values of the integers  $p, q$  ( $p$  and  $q$  relatively prime), the spectrum determined from Harper equation has a very complex structure. For instance, if  $p$  and  $q$  are chosen to belong to some infinite sequence such that, in the limit,  $p/q$  becomes arbitrarily close to an irrational number, the spectrum becomes a Cantor set (Hofstadter, 1976) and the wave functions exhibit self-similar behavior (Kohmoto, 1983). Even if the problem is restricted to commensurate flux only, the spectrum has energy gaps that, as  $q$  is increased, exhibit a hierarchical structure.

### *Hall conductance*

We now turn to the far less trivial question of computing the value of Hall conductance. Let us derive a version of the NiuThoulessWu formula for the case of a tight-binding system. In the case of a tight-binding system, the current operator  $J(x, y)$  flowing on the link  $\vec{r} \rightarrow \vec{r} + 1$  can be obtained by differentiation of the Hamiltonian  $J_\alpha(\vec{r}) = \frac{\partial H}{\partial A_\alpha}$ . In the case of a system coupled to an external electric field, the vector potential gets shifted. It is easy to show that, when electric is not zero, the kinetic part of the one-particle Hamiltonian  $h_{kin}$  takes the form

$$H(k_x, k_y) \rightarrow H(k_x + \theta_x, k_y + \theta_y), \quad (41)$$

where the external uniform electric field  $\mathbf{E}$  (or a twist  $\theta_\alpha(et/\hbar)E_\alpha$  is equivalent to a shift of the momentum of each particle by  $(et/\hbar)E$ . The Kubo formula can be written in the following simple form

$$\sigma_{xy} = \frac{e^2}{\hbar} \sum_n \varepsilon_{ab} \int_{BZ} d^2k \frac{\partial}{\partial k_a} \langle n | \frac{\partial}{\partial k_b} | n \rangle \quad (42)$$

The one-particle states  $n$  are labeled by a band index  $r$  ( $1 \leq r \leq q - 1$ ) and by a momentum label  $(k_x, k_y)$ , where  $k_x, k_y$  lies in the magnetic Brillouin zone.

### Haldane Honeycomb Model

In the late 1980s Haldane wanted to mimic the integer quantum Hall effect seen in the Landau-level problem while keeping the (full, not magnetic) translational symmetry of the lattice. This is actually rather hard to do because, as we saw, magnetic fields with nonzero flux per plaquette enlarge the unit cell. The unbroken translational symmetry of the lattice is equivalent to having zero (mod  $2\pi$ ) flux per plaquette, which leads us to the rather paradoxical situation of trying to obtain Landau levels without a nonzero magnetic field. Haldane realized that time-reversal breaking, rather than overall nonzero flux per unit cell, is the essential ingredient of a nonzero Hall conductance. To keep the translational symmetry of the lattice, we need to break time reversal without a net flux per plaquette. The easiest way to do this is to put the magnetic phases on the next-nearest neighbors because going

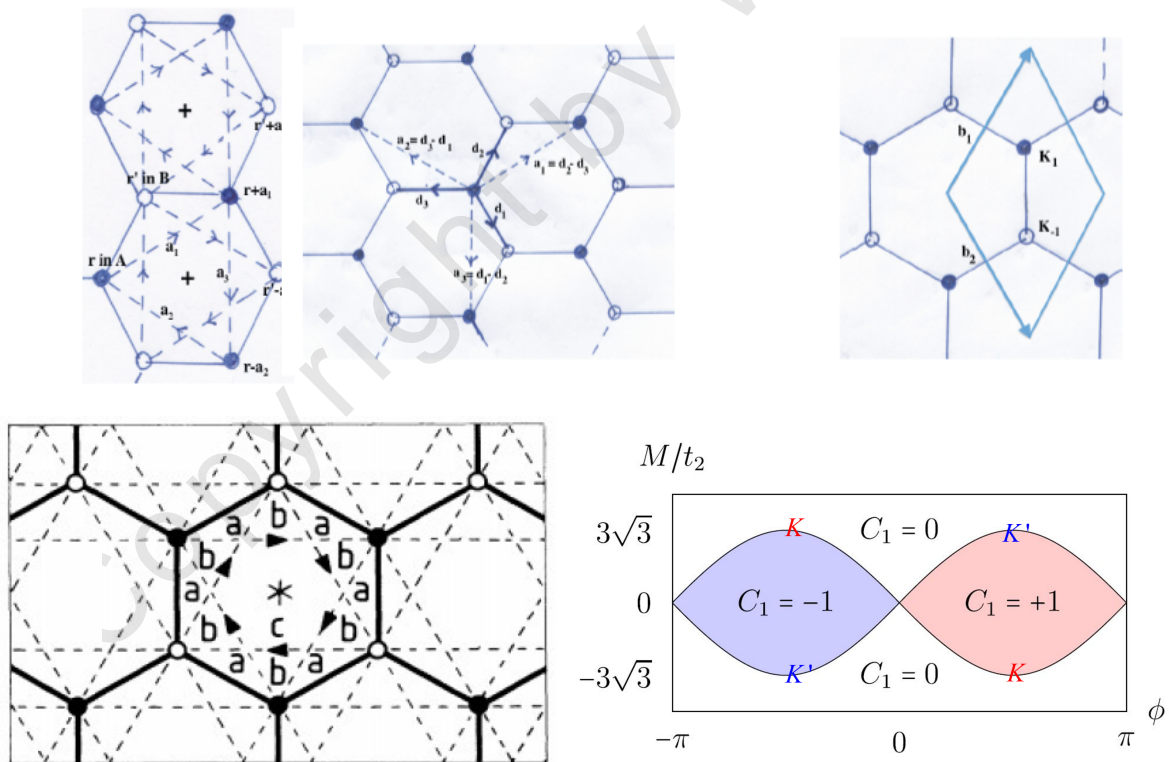


FIG. 6: The Haldane model. The honeycomb lattice, the magnetic fluxes in the Haldane model, and the associated reciprocal lattice with a possible choice of a rhombic Brillouin Zone

around a plaquette will not induce any nearest-neighbor phases. The Haldane model is on the honeycomb lattice, and the Hamiltonian is

$$H = \sum_{\langle ij \rangle} t a_i^\dagger a_j + \sum_{\langle\langle ij \rangle\rangle} t_2 e^{i\nu_{ij}\phi} a_i^\dagger a_j + \sum_i \epsilon_i M a_i^\dagger a_i \quad (43)$$

where  $\epsilon_i = \pm 1$ , depending on whether  $i$  is on the A or B sublattice,  $M$  is an on-site inversion symmetry-breaking term, and  $t$  is the nearestneighbor- hopping energy, and the next-nearest neighbor terms are defined in Fig. 6.

We choose the vectors are:

$$\mathbf{a}_1 = \begin{pmatrix} \sqrt{3}/2 \\ 1/2 \end{pmatrix}, \mathbf{a}_2 = \begin{pmatrix} -\sqrt{3}/2 \\ 1/2 \end{pmatrix}, \mathbf{a}_3 = \begin{pmatrix} 0 \\ -1 \end{pmatrix} = -(\mathbf{a}_1 + \mathbf{a}_2) \quad (44)$$

$$\mathbf{b}_1 = \mathbf{a}_2 - \mathbf{a}_3 = \begin{pmatrix} -\sqrt{3}/2 \\ 3/2 \end{pmatrix}, \mathbf{b}_2 = \mathbf{a}_3 - \mathbf{a}_1 = \begin{pmatrix} -\sqrt{3}/2 \\ -3/2 \end{pmatrix}, \mathbf{b}_3 = \mathbf{a}_1 - \mathbf{a}_2 = \begin{pmatrix} -\sqrt{3} \\ 0 \end{pmatrix} \quad (45)$$

Set  $\mathbf{b}_1, \mathbf{b}_2$  as two base vectors, then the reciprocal lattice spanned by  $\mathbf{G}_1, \mathbf{G}_2$  with  $\mathbf{b}_i \cdot \mathbf{G}_j = 2\pi\delta_{ij}$ , that is  $\mathbf{G}_1 = 2\pi \begin{pmatrix} -1/\sqrt{3} \\ 1/3 \end{pmatrix}, \mathbf{G}_2 = 2\pi \begin{pmatrix} -1/\sqrt{3} \\ -1/3 \end{pmatrix}$ . We define  $\mathbf{K} = \frac{1}{3}(\mathbf{G}_1 + \mathbf{G}_2) = \begin{pmatrix} -4\sqrt{3}\pi/9 \\ 0 \end{pmatrix}, \mathbf{K}' = -\mathbf{K}$ .

Use  $a_{iA} = \frac{1}{\sqrt{N}} \sum_k a_{kA} e^{i\mathbf{k} \cdot \mathbf{R}_{iA}}, a_{iB} = \frac{1}{\sqrt{N}} \sum_k a_{kB} e^{i\mathbf{k} \cdot \mathbf{R}_{iB}}$ ,  $N$  is the number of unit cell. Then we can get:

$$H = \sum_k \begin{pmatrix} a_{kA}^\dagger & a_{kB}^\dagger \end{pmatrix} H(k) \begin{pmatrix} a_{kA} \\ a_{kB} \end{pmatrix} \quad (46)$$

, and

$$H_{AA} = \langle kA | H_0 | kA \rangle = \frac{1}{N_A} \sum_{i,i'} e^{i\vec{k}(r_{iA} - r_{i'A})} \langle iA | H_0 | i'A \rangle = \varepsilon_A + t_2 \sum_i \cos(\phi + \vec{k}\vec{b}_i) \quad (47)$$

$$H_{BB} = \langle kB | H_0 | kB \rangle = \frac{1}{N_B} \sum_{j,j'} e^{i\vec{k}(r_{jA} - r_{j'A})} \langle jB | H_0 | j'B \rangle = \varepsilon_B + t_2 \sum_i \cos(-\phi + \vec{k}\vec{b}_i) \quad (48)$$

$$\begin{aligned} H_{BA} &= \langle kB | H_0 | kA \rangle = \frac{1}{N_A} \sum_{i,j} e^{i\mathbf{k} \cdot (\mathbf{r}_{iA} - \mathbf{r}_{jB})} \langle jB | H_0 | iA \rangle = \frac{1}{N_A} \sum_{\langle ij \rangle} e^{i\mathbf{k} \cdot (\mathbf{r}_{iA} - \mathbf{r}_{jB})} t_{ij} \\ &= t(e^{i\mathbf{k} \cdot \mathbf{a}_1} + e^{i\mathbf{k} \cdot \mathbf{a}_2} + e^{-i\mathbf{k} \cdot (\mathbf{a}_1 + \mathbf{a}_2)}) = t(\cos 2y + 2 \cos x \cos y) + it(2 \sin y \cos x - \sin 2y) = h_x + ih_y \end{aligned}$$

$$H_{AB} = H_{BA}^* \quad (49)$$

where  $x = k_x\sqrt{3}a/2$  and  $y = k_y a/2$ . Here we consider both sublattice A and B share the same coordinates in real space. To sum up,

$$H(k) = h_0\sigma_0 + \mathbf{h} \cdot \boldsymbol{\sigma} \quad (50)$$

$$h_0 = 2t_2 \cos \phi \sum_i \cos \mathbf{k} \cdot \mathbf{b}_i \quad (51)$$

$$h_x = t \sum_i \cos \mathbf{k} \cdot \mathbf{a}_i \quad (52)$$

$$h_y = -t \sum_i \sin \mathbf{k} \cdot \mathbf{a}_i \quad (53)$$

$$h_z = M + 2t_2 \sin \phi \sum_i \sin \mathbf{k} \cdot \mathbf{b}_i \quad (54)$$

Because of the  $C_3$  symmetry, the Dirac cone can only happen at  $K, K'$ . At the vicinity of  $K, K'$ , we have

$$H(K + q) = -3t_2 \cos \phi + \frac{3}{2}t_1(q_x\sigma_x - q_y\sigma_y) + (M + 3\sqrt{3}t_2 \sin \phi)\sigma_z \quad (55)$$

$$H(K' + q) = -3t_2 \cos \phi - \frac{3}{2}t_1(q_x\sigma_x - q_y\sigma_y) + (M - 3\sqrt{3}t_2 \sin \phi)\sigma_z \quad (56)$$

where  $-\pi < \phi < \pi$ . Here we used that,

$$\mathbf{K}_+ \cdot \mathbf{a}_1 = 2\pi/3, \mathbf{K}_+ \cdot \mathbf{a}_2 = -2\pi/3, \mathbf{K}_+ \cdot \mathbf{a}_3 = 0 \quad (57)$$

$$e^{i(\mathbf{K}_++q)\cdot\mathbf{a}_1} + e^{i(\mathbf{K}_++q)\cdot\mathbf{a}_2} + e^{i(\mathbf{K}_++q)\cdot\mathbf{a}_3} = e^{i2\pi/3}e^{i\mathbf{q}\cdot\mathbf{a}_1} + e^{i2\pi/3}e^{i\mathbf{q}\cdot\mathbf{a}_2} + e^{i\mathbf{q}\cdot\mathbf{a}_3} \quad (58)$$

$$\approx \frac{3}{2}q_x - \frac{3}{2}iq_y \quad (59)$$

$$\sum_j \sin \mathbf{K}_\pm \cdot \mathbf{b}_j = \pm 3\sqrt{3}/2 \quad (60)$$

### Graphene (without $t_2$ )

We first discuss the physics at  $t_2 = 0, M = 0$  first, which relates to famous graphene. A special feature of graphene is that the conduction and valence band touch each other in points  $K_\pm$  forming Dirac points. At these points all coefficients of  $h_\alpha = 0$  thus  $h$  can be linearly expanded around  $\mathbf{q} = \mathbf{k} - \mathbf{K}_\pm$  for small  $k$  resulting in  $h(\mathbf{q}) \approx v_F \mathbf{q}$ . Substituting the previous expression into H results in a Hamiltonian equivalent to the massless Dirac Hamiltonian  $H(\mathbf{q}) \approx v_F \mathbf{q} \cdot \boldsymbol{\sigma}$ , where  $v_F = 3ta/2$  is the Fermi velocity. This Hamiltonian was found by Dirac to describe relativistic particles quantum mechanically, the massless Dirac



Hamiltonian thus describes a massless relativistic particle which has a linear energy dispersion with respect to  $q$ .

Haldane's insight was that by breaking P or T the Dirac point opens up due to  $h_z$  this is possible because the symmetry constraints no longer have to be satisfied both.  $H = \pm v_F \mathbf{q} \cdot \boldsymbol{\sigma} + m\sigma_z$ . There are two cases to consider. In one case, when P symmetry is broken, then the Dirac point gains a mass  $m = h_z(K_+)$  and T symmetry requires  $m' = h_z(K_-)$  thus both Dirac points have mass  $m$ . In the other case, when T symmetry is broken P symmetry requires  $m = h_z(K)$  and  $m' = h_z(K)$  thus  $m' = -m$ . In this case H changes from the north to the south pole across the BZ covering  $S_2$  and the subtended solid angle  $4\pi$  resulting in a Chern number of  $C = 1$ .

*Symmetries*

*Chern number*

We restrict ourselves to the case of a one-particle Hamiltonian  $H$  having Bloch eigenvalues  $\epsilon_{nk}$  and eigenstates  $|\psi_{nk}\rangle$ . The cell-periodic part of the Bloch function  $u_{nk}(r) = e^{-ik \cdot r} \psi_{nk}(r)$  is then an eigenfunction of the effective Hamiltonian  $H(k) = e^{-ik \cdot r} H e^{ik \cdot r}$ . We consider electrons to be spinless, but factors of two can easily be inserted for non-interacting spin channels.

We can now define the Chern invariant[?] for an insulator, defined here as a system with a gap in the single-particle density of states separating occupied and unoccupied states,

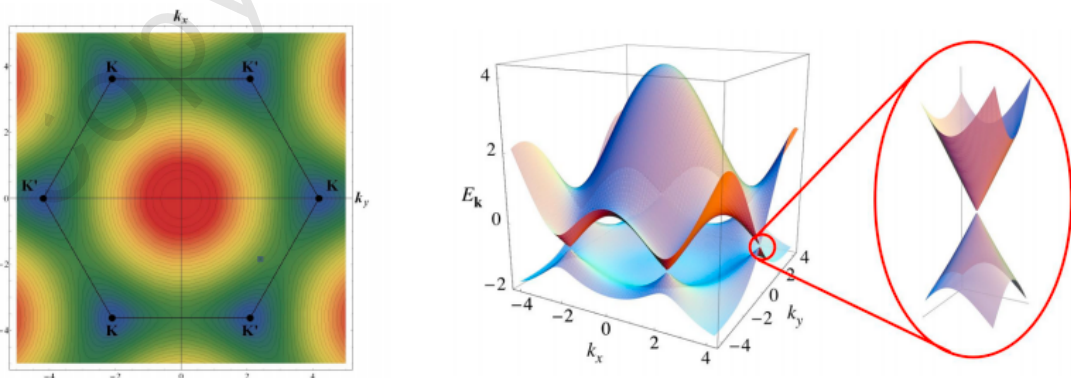


FIG. 7: Band structure of graphene.

to be

$$\mathbf{C} = \frac{i}{2\pi} \int_{\text{BZ}} \sum_n^{\text{occ}} \partial_k u_{nk} \times \partial_k u_{nk}, \quad (61)$$

where BZ denotes an integral over the Brillouin zone and  $\partial k = \partial/\partial k$ . The cross product notation in Eq. (61) implies, for example, that  $C_z$  contains terms involving  $i p \partial_{k_x} u_{nk} \partial_{k_y} u_{nk} - i p \partial_{k_y} u_{nk} \partial_{k_x} u_{nk}$ . For non-interacting electrons, [?] the Chern invariant is quantized in units of reciprocal-lattice vectors  $G$ . For the case of a two-dimensional system with only a single occupied band, Eq. (61) becomes

$$C = \frac{i}{2\pi} \int_{\text{BZ}} k \langle \partial_k u_k | \times | \partial_k u_k \rangle. \quad (62)$$

In two dimensions the Chern invariant is a pseudo-scalar called the Chern number which can only take integer values. Alternatively, we can write the Chern number in terms of the Berry connection  $A(k) = i u_k \partial_k u_k$  and the Berry curvature  $\Omega(k) = \nabla_k \times A(k)$  as

$$C = \frac{1}{2\pi} \int_{\text{BZ}} k \Omega(k) = \frac{1}{2\pi} \oint_{\text{BZ}} d k \cdot A(k). \quad (63)$$

A Chern insulator is now simply defined as an insulator with a nonzero Chern invariant. Conversely, we define a normal insulator to be an insulator with zero Chern invariant. Hence, the NI/CI transition is characterized by a change of the Chern invariant from zero to a nonzero value.

The Chern invariant of Eqs. (61) and (62) is gauge invariant, [?] i.e., invariant with respect to the choice of phases of the  $|u_{nk}\rangle$ , or in the more general multiband case, the choice of unitary rotations applied to transform the occupied states among themselves at a given  $k$ . It can be shown that in normal insulators it is always possible to make a gauge choice such that the Bloch orbitals are periodic in  $k$ -space (i.e.,  $|\psi_{n, k+G}\rangle = |\psi_{nk}\rangle$ ) and smooth in  $k$  (i.e., continuous and differentiable), whereas no such choice is possible for a Chern insulator.

Consider the noninteracting two-band Bloch Hamiltonian of the generic form

$$H_0 := \sum_{k \in \text{BZ}} \psi_k^\dagger \mathcal{H}_k \psi_k, \quad \mathcal{H}_k := h_{0,k} \sigma_0 + \mathbf{h}_k \cdot \boldsymbol{\sigma}. \quad (64a)$$

Here, BZ stands for the Brillouin zone,  $\psi_k^\dagger = (c_{k,A}^\dagger, c_{k,B}^\dagger)$ , where  $c_{k,s}^\dagger$  creates a Bloch state on sublattice  $s = A, B$ , and the  $2 \times 2$  matrices  $\sigma_0$  and  $\boldsymbol{\sigma}$  are the identity matrix and the

three Pauli matrices acting on the sublattice indices. If we define

$$\mathbf{h}_k := \frac{\mathbf{h}_k}{|\mathbf{h}_k|}, \quad \tan \phi_k := \frac{\widehat{h}_{2,k}}{\widehat{h}_{1,k}}, \quad \cos \theta_k := \widehat{h}_{3,k}, \quad (64b)$$

we can write the eigenvalues of Hamiltonian  $\mathcal{H}_k$  as  $\varepsilon_{\pm,k} = h_{0,k} \pm |\mathbf{h}_k|$  and for the corresponding orthonormal eigenvectors

$$\chi_{+,k} = \begin{pmatrix} e^{-i\phi_k/2} \cos \frac{\theta_k}{2} \\ e^{+i\phi_k/2} \sin \frac{\theta_k}{2} \end{pmatrix}, \quad \chi_{-,k} = \begin{pmatrix} e^{-i\phi_k/2} \sin \frac{\theta_k}{2} \\ -e^{+i\phi_k/2} \cos \frac{\theta_k}{2} \end{pmatrix}. \quad (64c)$$

The two eigenvectors are exactly the two spinors we have discussed for the spin-1/2 problem, for which the story of the choice of the phase and the unavoidable presence of vortex singularities applies as well.

The Chern numbers for the bands labeled by  $\pm$  in Eq. (64c) are given by

$$C_{\pm} = \mp \int_{\mathbf{k} \in BZ} \frac{d^2 \mathbf{k}}{4\pi} \epsilon_{\mu\nu} \left[ \partial_{k_\mu} \cos \theta(\mathbf{k}) \right] \left[ \partial_{k_\nu} \phi(\mathbf{k}) \right]. \quad (65)$$

They have opposite signs if nonzero. All the information about the topology of the Bloch bands of a gaped system is encoded in the single-particle wave functions. For example, the Chern numbers depend solely on the eigenfunctions. Haldane's model and the chiral- $\pi$ -flux are topologically equivalent in the sense that both have two bands with Chern numbers  $\pm 1$ .

We calculate the Chern number, it depends on the sign of  $h_z$ :

$$C = -\frac{1}{2} \text{sign}((M - 3\sqrt{3}t_2 \sin \phi)) + \frac{1}{2} \text{sign}((M + 3\sqrt{3}t_2 \sin \phi)) \quad (66)$$

and we get the phase diagram below. In this phase diagram Fig.6, we derive an interesting statement: Gap closings are sources of Berry curvature. The situation is explained by the following sketch, which also gives a bird's-eye view of the phase diagram of the Haldane model as a function of the ratio  $t_2/M$ ,  $\phi = \pi/2$ , as shown in Fig.8. We find band degeneracies at the  $\mathbf{k}$  points where  $\mathbf{h}(k) = 0$ : When  $M = 0$  and  $\phi = 0$ , the standard graphene case (where one usually puts  $t_2 = 0$  as well), these degeneracies occur at the two famous Dirac points  $\mathbf{K}_{\pm}$ . And we have  $\mathbf{K}_{\pm} \cdot \mathbf{a}_j = \mp 2\pi/3$ . At the two Dirac points (and only at those points!) one has  $h_x(\mathbf{K}_{\pm}) = 0$  and  $h_y(\mathbf{K}_{\pm}) = 0$ . Since the presence of a degeneracy requires/implies  $\mathbf{h}(k) = 0 \rightarrow h_x = h_y(k) = 0$ , we immediately conclude that a degeneracy can only occur in one of the two BZ corners  $\mathbf{K}_{\pm}$ . The matter is then decided by what is the value of  $h_z(\mathbf{K}_{\pm})$ .

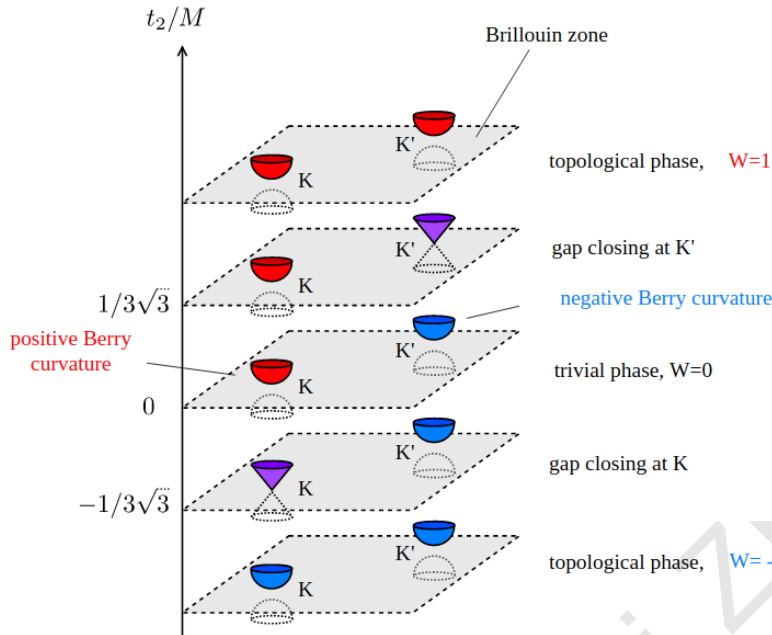


FIG. 8: A schematic illustration of the energy spectrum close to the Dirac points in the Brillouin zone, for some representative values of  $t_2/M$  (for simplicity we drew the Brillouin zone as a square and not a hexagon, but that's not essential). The two massless Dirac cones appearing for the critical points are the sources of the Berry curvature, which then spreads along the vertical axis, passing through the Brillouin zones of the gapped phases. At  $t_2 = 0$  Brillouin zone is sandwiched between the two gap closings: it has opposite curvature for the two Dirac points, and a total Chern number of zero. The Brillouin zones for  $|t_2| > M/(3\sqrt{3})$ , on the other hand, have Berry curvature with the same sign for both Dirac points, and a total Chern number equal to  $\pm 1$ .

Since  $\sum_j \sin \mathbf{K}_\pm \cdot \mathbf{b}_j = \mp 3\sqrt{3}/2$ , we see that the presence of degeneracies is all linked to  $h_z(\mathbf{K}_\pm) = M + \pm t_2 3\sqrt{3} \sin \phi = 0$ . These two equations, define two curves in the  $M/t_2$  versus  $\phi$  plane, the phase diagram of the Haldane model, where the gap closes either at the  $\mathbf{K}_+$  point, when  $M/t_2 = 3\sqrt{3} \sin \phi$ , or at the  $\mathbf{K}_-$  point, when  $M/t_2 = -3\sqrt{3} \sin \phi$ . Everywhere else in the phase diagram a gap is present, and the system is therefore an insulator.

Next, we provide some more detailed discussion on the Chern number and phase diagram. On one hand, let us re-express the eigenvectors as  $|u(\mathbf{k})\rangle$  by  $|u(\mathbf{h}(\mathbf{k}))\rangle$  (note that we make mapping between Torus and Sphere), to make the connection between the current problem

and the spin-1/2 problem that we studied before.

$$u_{+,k} = \frac{1}{2h(h+h_z)} \begin{pmatrix} h_z + h \\ h_x - ih_y \end{pmatrix}, u_{-,k} = \frac{1}{2h(h-h_z)} \begin{pmatrix} h_z - h \\ h_x - ih_y \end{pmatrix} \quad (67)$$

where  $h = |\mathbf{h}_k|$  and eigenvalue is  $E_{\pm} = \pm h = \pm\sqrt{h_x^2 + h_y^2 + h_z^2}$ . The Berry connection and curvature is

$$A_i(\mathbf{k}) = i\langle\chi_-|\nabla_i|\chi_-\rangle = -\frac{1}{2h(h+h_z)}[h_y\partial_i h_x - h_x\partial_i h_y] \quad (68)$$

$$B_{ij} = \frac{1}{2h^3}\epsilon_{abc}h_a\partial_i h_b\partial_j h_c \quad (69)$$

The berry curvature becomes

$$i[\langle\partial_{k_x}u(\mathbf{k})|\partial_{k_y}u(\mathbf{k})\rangle - \langle\partial_{k_y}u(\mathbf{k})|\partial_{k_x}u(\mathbf{k})\rangle] = i\sum_{ij}\langle\partial_{h_i}u(\mathbf{h})|\partial_{h_j}u(\mathbf{h})\rangle\det\begin{pmatrix} \partial_{k_x}h_i & \partial_{k_y}h_j \\ \partial_{k_x}h_j & \partial_{k_y}h_i \end{pmatrix} \quad (70)$$

$$= \sum_{i<j}F_{ij}(\mathbf{h})J_{ij}(k) \quad (71)$$

$$F_{ij}(\mathbf{h}) = i[\langle\partial_{h_i}u(\mathbf{h})|\partial_{h_j}u(\mathbf{h})\rangle - \langle\partial_{h_j}u(\mathbf{h})|\partial_{h_i}u(\mathbf{h})\rangle] = \epsilon^{ijk}\frac{h_k}{2h^3} \quad (72)$$

$$\int_{BZ} dk_x dk_y \sum_{i<j} F_{ij}(\mathbf{h})J_{ij}(k) = \frac{1}{2\pi} \int_{BZ} dk_x dk_y \frac{1}{h^3} \mathbf{h} \cdot \left( \frac{\partial \mathbf{h}}{\partial k_x} \times \frac{\partial \mathbf{h}}{\partial k_y} \right) = C \quad (73)$$

Here, let us try to discuss this result. Fig.9 shows, for instance, how the closed surface  $\mathbf{h}(k)$  looks like when  $k$  in BZ, for trivial insulator and chern insulator in the phase diagram. For a trivial insulator, (left

figures), the origin  $\mathbf{h} = 0$  outside the surface, while for a topological insulator, (right figure), the origin  $\mathbf{h} = 0$  inside the surface. For the case that the Haldane's spaceship  $h(k)$  lies all away and outside from the origin  $h = 0$  of the monopole field. Then you expect that the total Berry flux through this closed surface outside the singularity is exactly 0, and you obtain  $C = 0$ . When the Haldane's spaceship encloses the singularity at  $h = 0$ , then the solid angle through which the Berry flux goes is  $4\pi$ , but the monopole charge is  $1/2$ , therefore you expect  $c = 1$ .

On the other hand, we focus on the discussion of  $u_{-,k}$  first and the discussion on the other one is similar. There is a singular, if  $h_x = h_y = 0$  and  $h_z > 0$ :

$$u_{-,k}^I = \frac{1}{2h(h-h_z)} \begin{pmatrix} h_z - h \\ h_x - ih_y \end{pmatrix} = \frac{1}{2h(h-h_z)} \begin{pmatrix} 0 \\ 0 \end{pmatrix} \quad (74)$$

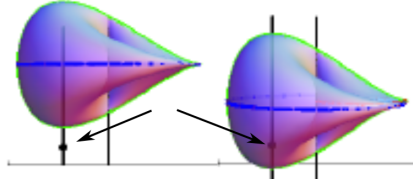


FIG. 9: The Haldane spaceship  $\mathbf{h}(k)$  when  $\mathbf{k}$  spans the BZ, for the trivial (left) and topological (right) insulator. Arrow marks the zero point  $\mathbf{h} = 0$ .

In fact, there is another way to write down the same eigenvector (a global phase shift):

$$u_{-,k}^{II} = \frac{1}{2h(h-h_z)} \begin{pmatrix} h_z - h \\ h_x - ih_y \end{pmatrix} \frac{\frac{h_z+h}{h_x-ih_y}}{\left| \frac{h_z+h}{h_x-ih_y} \right|} = \frac{1}{2h(h-h_z)} \frac{1}{\left| \frac{h_z+h}{h_x-ih_y} \right|} \begin{pmatrix} \frac{-h_x^2-h_y^2}{h_x-ih_y} \\ h_z + h \end{pmatrix} \quad (75)$$

The two wavefunctions  $u^I$  and  $u^{II}$  differ by a phase:  $u^{II} = u^I e^{i\phi_k}$ . This new wavefunction  $u^{II}$  is well defined at  $h_x = h_y = 0$  and  $h_z > 0$ . However, it is NOT well defined at  $h_x = h_y = 0$  and  $h_z < 0$ .

Setting  $0 < \phi < \pi$ :

- $M < -3\sqrt{3}t_2 \sin \phi$ : Both  $K_{\pm}$  have  $h_z < 0$ , we can choose  $u^I$  that is always smooth in whole BZ, therefore, the total Berry curvature should be zero.
- $-3\sqrt{3}t_2 \sin \phi < M < 3\sqrt{3}t_2 \sin \phi$ :  $h_z < 0$  at  $K_+$  and  $h_z > 0$  for the other  $K_-$ . Therefore, we need two wavefunctions. First, we draw a small circle around the  $K_+$ . Inside this small circle, which we will call region  $D_I$ , we use  $u^I$ . Otherwise, we use  $u^{II}$  outside  $D_I$ . And the Berry connection are related also by the same gauge transformation  $A^{II} = A^I + \nabla \phi_k$ . The total Berry curvature is  $\int_{BZ} dk B(k) = \oint_{D_I} \nabla \times A^I + \oint_{D_{II}} \nabla \times A^{II} = \oint_{\partial D_I} dk \cdot A^I + \oint_{\partial D_{II}} dk \cdot A^{II} = \oint_{\partial D_I} dk \cdot (A^I - A^{II}) = \oint_{\partial D_I} dk \cdot \nabla \phi_k = \int_0^{2\pi} d\phi = 2\pi$ .
- $M > 3\sqrt{3}t_2 \sin \phi$ : Both  $K_{\pm}$  have  $h_z > 0$ , we can choose  $u^{II}$  that is always smooth in whole BZ, therefore, the total Berry curvature should be zero.

The Berry phase can only be computed if the Hamiltonian has a gap. For a Hamiltonian, this means that we can compute the Chern number only for an isolated band which does not touch any other band. If there is a band touching, the Berry phase is undefined.

Remarks: 1. The model of Haldane is the first example of a topological state beyond quantum Hall effect. It demonstrates that topological state is a generic concept, which may

appear in any insulating systems (NOT just quantum Hall). 2. It also demonstrates that as long as the topological index is nonzero, one will observe all the topological phenomena expected for a quantum Hall state, including the quantized Hall conductivity and the existence of the edge states. 3. The key differences between the model of Haldane and the quantum Hall effects are (1) the B field is on average zero in the model of Haldane while the QHE has a uniform B field and (2) there is a very strong lattice background in the model of Haldane while the QHE requires weak lattice potential. 4 Systems similar to the Haldanes model are known as topological Chern insulators or Chern insulators (average B is 0 and have a strong lattice potential).

Copyright by Weizi

## TWO-DIMENSIONAL TIME-REVERSAL TOPOLOGICAL INSULATORS

In Chern insulators, time-reversal symmetry is broken by magnetic field (flux). time-reversal symmetric (or time-reversal invariant) two-dimensional insulator was first introduced by C. Kane and G. Mele in 2005.

### Time Reversal Symmetry

In the field of topological insulators, we are in the business of unraveling the effect that the presence (or absence) of continuous and discrete symmetries has on the physics of materials.

Time -reversal (TR) symmetry is a fundamental property: systems behave quite differently depending on whether or not they exhibit time reversal. Time reversal is a transformation that reverses the arrow of time:  $t \rightarrow -t$ . in 2005 by Kane and Mele, we now understand that analyzing TR-invariant systems can be equally rewarding: even though, as we show next, these systems cannot exhibit Hall effects, they can, nevertheless, exhibit other equally interesting topological phenomena, such as the nontrivial Z2 topological classification.

Here we present a detailed account of TR symmetry for both spinful and spinless particles, of its action on operators and Bloch Hamiltonians, and of its implications on the Berry potential and Berry curvature. We introduce time reversal as a symmetry T of the Hamiltonian H of a system:

$$[T, H] = 0 \tag{76}$$

#### *Spinless particle*

The TR operator changes only the arrow of time. As such, it leaves the position operator  $x$  unchanged in particular, time reversal commutes with any spatial symmetry. However, it flips the sign of the momentum operator  $p$  because it is proportional to the velocity, a time derivative of a TR-invariant quantity (the position operator):

$$TxT^{-1} = x, \quad T\hat{p}T^{-1} = -\hat{p} \tag{77}$$

We would like to find the representation of the TR operator. By looking at the action of time reversal on the commutator of  $x$  and  $p$ ,

$$T[x, p]T^{-1} = T i\hbar T^{-1} = -i\hbar \tag{78}$$



which gives

$$TiT^{-1} = -i \quad (79)$$

The preceding makes it clear that the TR operator must be proportional to the operator of complex conjugation. Such operators are called anti-unitary and, unlike operators, do not have eigenvalues. For a particle without spin, the story ends here because the Hilbert space can be made out of scalars; hence,

$$T = K \quad (80)$$

where K is the complex-conjugation operator. Thus we have  $T^2 = 1$  for spinless.

We would now like to analyze the consequences that time reversal has for Bloch Hamiltonians. For spinless particles, T leaves the on-site creation operators unchanged

$$Tc_jT^{-1} = c_j \quad (81)$$

where we can add any orbital indices to the creation operators as long as the index is not spin. But, in momentum space, it leads to

$$Tc_kT^{-1} = c_{-k} \quad (82)$$

, due to the Fourier transformation properties.

We are now ready to obtain the transformation of a Bloch Hamiltonian under time reversal. For a TR-invariant Hamiltonian, we then have

$$THT^{-1} = T \sum_k c_k^\dagger h(k) c_k T^{-1} = \sum_k c_{-k}^\dagger Th(k) T^{-1} c_{-k} = H = \sum_k c_{-k}^\dagger h(-k) c_{-k} \quad (83)$$

which leads to

$$Th(k)T^{-1} = h(-k) \quad (84)$$

*Remark.* Spinless systems with T symmetry cannot exhibit nonzero Hall conductance.

As an example, we consider a single band  $|u(k)\rangle$  below the Fermi level, the generalization to multiple bands is obvious. The berry curvature is

$$\begin{aligned} F_{ij}(-k) &= -i[\langle \partial_i u(-k) | \partial_j u(-k) \rangle - h.c] \\ &= -i[\partial_i u^*(-k) \partial_j u(-k) - h.c] \end{aligned} \quad (85)$$

With the help of relation  $u(-k) = Tu(k) = u^*(k)$  from the time-reversal symmetry [ $Tu(k) = u^*(-k) = u(k)$ ], we have

$$\begin{aligned} F_{ij}(-k) &= -i[\partial_i u^*(-k)\partial_j u(-k) - h.c] \\ &= -i[\partial_i u(k)\partial_j u^*(k) - h.c] = -F_{ij}(k) \end{aligned} \quad (86)$$

which then gives zero upon integration over the BZ.

### *Spinful particle*

We now look at particles with internal angular momentum, or spin,  $\mathbf{S}$ . This requires an extra action of the time-reversal operator; because angular momentum is itself a momentum, it is odd under time reversal

$$TST^{-1} = -\mathbf{S} \quad (87)$$

This implies that the spin flips its direction under time reversal. We can represent this action by a rotation by  $\pi$  around some arbitrary axis. [If we use the normal choice of Pauli matrix, i.e.  $\mathbf{S} = \hbar/2(\sigma_x, \sigma_y, \sigma_z)$ , the following definition can satisfy  $TST^{-1} = -\mathbf{S}$ . If the components of  $\mathbf{S}$  are  $x, z$ , the complex conjugation does nothing, but the matrix  $\sigma_y$  anticommutes with  $\sigma_{x,z}$ ] With the choice of the rotation axis as  $y$ , the form of the TR operator is fixed:

$$T = e^{-i\pi S_y} K = -i\sigma_y K. \quad (88)$$

Then we have

$$T^2 = -i\sigma_y K(-i\sigma_y K) = \sigma_y \sigma_y^* K K = -1 \quad (89)$$

This is different from the spinless case.

We now want to obtain the action of the  $T$  operator on Bloch Hamiltonians of spin-half particles.

$$Tc_{i,\uparrow}T^{-1} = c_{i,\downarrow}, \quad Tc_{i,\downarrow}T^{-1} = -c_{i,\uparrow}, \quad Tc_{i,\sigma}T^{-1} = i(\sigma_y)_{\sigma\sigma'}c_{i,\sigma'} \quad (90)$$

This is special. One can understand it, by assuming  $Tc_{\uparrow}T^{-1} = Ac_{\downarrow}$  and  $Tc_{\downarrow}T^{-1} = Bc_{\uparrow}$ . And check the operator  $Tc_{\uparrow}$  on  $c_{\uparrow}^{\dagger}|0\rangle$ .

We are interested in the transformation of the Bloch Hamiltonian, so we Fourier-transform the coefficients

$$Tc_{k,\uparrow}T^{-1} = c_{-k,\downarrow}, \quad Tc_{k,\downarrow}T^{-1} = -c_{-k,\uparrow}, \quad Tc_{k,\sigma}T^{-1} = i(\sigma_y)_{\sigma\sigma'}c_{-k,\sigma'} \quad (91)$$

and

$$\begin{aligned}
H &= THT^{-1} \\
\sum_{k,\alpha,\beta} c_{k,\alpha}^\dagger h_{\alpha\beta}(k) c_{k,\beta} &= T \left[ \sum_{k,\alpha,\beta} c_{k,\alpha}^\dagger h_{\alpha\beta}(k) c_{k,\beta} \right] T^{-1} \\
&= \sum_{k,\alpha,\beta} c_{-k,\alpha'}^\dagger i(\sigma_y)_{\alpha\alpha'}^T T h_{\alpha\beta}(k) T^{-1} i(\sigma_y)_{\beta'\beta} c_{-k,\beta'} \\
&= \sum_{k,\alpha,\beta} c_{k,\alpha}^\dagger i(\sigma_y)_{\alpha\alpha'}^T T h_{\alpha'\beta'}(-k) T^{-1} i(\sigma_y)_{\beta'\beta} c_{k,\beta} \tag{92}
\end{aligned}$$

thus we have

$$h_{\alpha\beta}(k) = i(\sigma_y)_{\alpha\alpha'}^T h_{\alpha'\beta'}^*(-k) i(\sigma_y)_{\beta'\beta} \tag{93}$$

Without matrix indices, it is written in the compact form

$$Th(k)T^{-1} = h(-k) \tag{94}$$

For a Bloch wavefunction of our Hamiltonian at momentum  $k$ ,  $|u^I(k)\rangle$  with energy  $E_k$

$$h(k)|u^I(k)\rangle = E_k|u^I(k)\rangle \tag{95}$$

then the wavefunction  $T|u^I(k)\rangle$  is an eigenstate of the same Hamiltonian at momentum  $k$ , with energy  $E(-k) = E(k)$ :

$$h(-k)|u(-k)\rangle = h(-k)T|u^I(k)\rangle = Th(k)T^{-1}T|u^I(k)\rangle = Th(k)|u^I(k)\rangle = TE_k|u^I(k)\rangle = E_kT|u^I(k)\rangle = E_kT|u^I(k)\rangle = E_kT|u^I(k)\rangle \tag{96}$$

At special points in the BZ, which are invariant (mod a reciprocal lattice vector) under time reversal (such as  $(0, 0)$ ,  $(\pi, 0)$ ,  $(0, \pi)$ ,  $(\pi, \pi)$  in two dimensions and similar ones in three dimensions we denote these special points as  $G/2$  in any dimension), the Bloch Hamiltonian is invariant under the TR transformation:  $Th(G/2)T^{-1} = h(G/2)$ ; hence,  $u(G/2)$  and  $Tu(G/2)$  have the same energy, resulting in a double degeneracy at these special points in the Brillouin zone. The double degeneracy is guaranteed by the fact that we know that the two states are orthogonal due to Kramers theorem. [And we can prove  $T|u(k)\rangle$  is a different state from  $|u(k)\rangle$ . Supposed that  $T|u\rangle = e^{i\phi}|u\rangle$ , we have  $T^2|u\rangle = Te^{i\phi}|u\rangle = e^{-i\phi}e^{i\phi}|u\rangle = |u\rangle$ , and thus  $T^2 = 1$ , which is against to our definition above. Therefore,  $T|u\rangle$  is a orthogonal state to  $|u\rangle$ .]

Exercises. Similar to the spinless case, an identical statement can be proved for half-integer fermions with time reversal: Chern number vanishes for time-reversal system. For

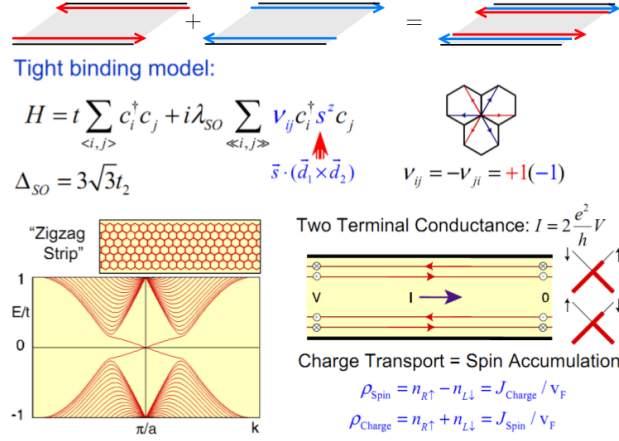


FIG. 10: The sketch of time-reversal symmetric insulator from Chern insulators

time-reversal spin-half system, we need at least two bands. The berry curvature is

$$F(k_x, k_y) = -i[\langle \partial_x u^I(k) | \partial_y u^I(k) \rangle - h.c.] - i[\langle \partial_x u^{II}(k) | \partial_y u^{II}(k) \rangle - h.c.] \quad (97)$$

Using the relation

$$\begin{aligned} \langle \partial_{-k_x} u^I(-k) | \partial_{-k_y} u^I(-k) \rangle &= - \langle \partial_x u^{II}(k) | \partial_y u^{II}(k) \rangle \\ \langle \partial_{-k_x} u^{II}(-k) | \partial_{-k_y} u^{II}(-k) \rangle &= - \langle \partial_x u^I(k) | \partial_y u^I(k) \rangle \end{aligned} \quad (98)$$

which immediately shows that the added curvature for these two bands satisfies

$$F(-k_x, -k_y) = -F(k_x, k_y) \quad (99)$$

This, in turn, forces the Chern number to vanish when integrated over the full BZ.

### Kane-Mele Model and Quantum Spin Hall Effect

There is a simple way to construct lattice systems with Time-Reversal Symmetry. Take as a starting point a lattice model of a d dimensional insulator, with a Hamiltonian  $H(k)$ . We define a time-reversal invariant new system by giving the Hamiltonian,

$$H_2(k) = \begin{pmatrix} H(k) & 0 \\ 0 & H^*(-k) \end{pmatrix} \quad (100)$$

$$TH_2(k)T^{-1} = i\tau_y K H_2(k) (-i\tau_y K) = \begin{pmatrix} 0 & 1 \\ -1 & 0 \end{pmatrix} \begin{pmatrix} H^*(-k) & 0 \\ 0 & H(k) \end{pmatrix} \begin{pmatrix} 0 & -1 \\ 1 & 0 \end{pmatrix} = H_2(k) \quad (101)$$

Here  $H^*$  denotes the complex conjugate of the matrix, an operation that is basis dependent, and  $KH(k)K = H^*(k)$ .

Following this method, we consider a double-layer Haldane model, which was first proposed by Kane and Mele in 2005:

$$H = \sum_{\langle ij \rangle} t c_i^\dagger c_j + \sum_{\langle\langle ij \rangle\rangle} t_2 e^{i\nu_{ij}} c_i^\dagger s_z c_j + \sum_i \epsilon_i M c_i^\dagger c_i \quad (102)$$

where we define  $c_i = (c_{i,\uparrow}, c_{i,\downarrow})$ . Please note that the Haldane phase takes opposite sign for different spins. Now in the momentum space, the Hamiltonian becomes a 4-band model,

$$H_2(k) = \begin{pmatrix} H_\uparrow(k) & 0 \\ 0 & H_\downarrow(k) \end{pmatrix} = \begin{pmatrix} H_1(k) & 0 \\ 0 & H_1^*(-k) \end{pmatrix} \quad (103)$$

$$H_1(k) = h_0 \sigma_0 + \mathbf{h} \cdot \boldsymbol{\sigma} \quad (104)$$

$$h_0 = 2t_2 \cos \phi \sum_i \cos \mathbf{k} \cdot \mathbf{b}_i \quad (105)$$

$$h_x = t \sum_i \cos \mathbf{k} \cdot \mathbf{a}_i \quad (106)$$

$$h_y = -t \sum_i \sin \mathbf{k} \cdot \mathbf{a}_i \quad (107)$$

$$h_z = M + 2t_2 \sin \phi \sum_i \sin \mathbf{k} \cdot \mathbf{b}_i \quad (108)$$

This model is easy to diagonalize and gives two copies of the Haldane model. To see the edge states, we diagonalize in a cylinder geometry that has open-boundary conditions on two edges. The energy gap is  $|3\sqrt{3}t_2 - M|$ . For  $M > 3\sqrt{3}t_2$ , the system is an inversion-symmetry-breaking dominated phase and, if diagonalized so that the edge is of zig-zag type, it will have edge modes connecting the cones (similar to the ones studied in the gapless graphene case, but in this case they will be dispersive), but they will not cross the bulk gap. In contrast, for  $M < 3\sqrt{3}t_2$ , we see that the system has edge modes crossing the bulk gap. There is a pair of counter-propagating edge modes on each edge.

Each edge has a pair of counterpropagating edge modes, which cross at some T-invariant point. This crossing is protected by T symmetry. As long as time reversal is preserved, every k-point in the system must have a T orthogonal counterpart at k. The T-invariant points must each have two states, by Kramers theorem. That means the gap can never open for a single pair of counterpropagating modes.

If  $S_z$  is a good quantum number, threading a flux through the system takes one spin  $\uparrow$  from the left edge, A, to the right edge, B, and takes spin  $\downarrow$  from edge B to edge A. Hence the system pumps quantized spin and has a quantized spinHall conductance of 2 (in units of  $e^2/h$ ). This is quantum spin Hall effect.

### Symmetries

According to the definition of time-reversal symmetry, we know

$$\hat{T} = i\sigma_y K : \quad \hat{T}a_{\mathbf{k},\sigma}^\dagger \hat{T}^{-1} = (-\sigma)a_{-\mathbf{k},-\sigma}^\dagger \quad (109)$$

so we also know that

$$\hat{T} : \quad \hat{T}a_{i,\sigma}^\dagger \hat{T}^{-1} = (-\sigma)a_{i,-\sigma}^\dagger \quad (110)$$

since we have

$$\hat{T}a_{i,\sigma}^\dagger \hat{T}^{-1} = \hat{T} \sum_{\mathbf{k}} e^{i\mathbf{k}\cdot\mathbf{r}_i} \hat{T}^{-1} \hat{T}a_{\mathbf{k},\sigma}^\dagger \hat{T}^{-1} = \sum_{\mathbf{k}} e^{-i\mathbf{k}\cdot\mathbf{r}_i} (-\sigma)a_{-\mathbf{k},-\sigma}^\dagger = (-\sigma)a_{i,-\sigma}^\dagger \quad (111)$$

According to the definition of inversion symmetry, we know

$$\hat{I} : \quad \hat{I}a_{\mathbf{k},\sigma}^\dagger \hat{I}^{-1} = b_{-\mathbf{k},\sigma}^\dagger, \quad \hat{I}b_{\mathbf{k},\sigma}^\dagger \hat{I}^{-1} = a_{-\mathbf{k},\sigma}^\dagger \quad (112)$$

so we also know that

$$\hat{I} : \quad \hat{I}a_{i,\sigma}^\dagger \hat{I}^{-1} = b_{-i,\sigma}^\dagger, \quad \hat{I}b_{i,\sigma}^\dagger \hat{I}^{-1} = a_{-i,\sigma}^\dagger \quad (113)$$

since we have

$$\hat{I}a_{i,\sigma}^\dagger \hat{I}^{-1} = \hat{I} \sum_{\mathbf{k}} e^{i\mathbf{k}\cdot\mathbf{r}_i} \hat{I}^{-1} \hat{I}a_{\mathbf{k},\sigma}^\dagger \hat{I}^{-1} = \sum_{\mathbf{k}} e^{i\mathbf{k}\cdot\mathbf{r}_i} b_{-\mathbf{k},\sigma}^\dagger = b_{-i,\sigma}^\dagger \quad (114)$$

Here we used the condition  $\hat{I}\mathbf{r}\hat{I}^{-1} = -\mathbf{r}$  and  $\hat{I}\mathbf{k}\hat{I}^{-1} = -\mathbf{k}$ .

1. Time-Reversal symmetry with  $t_1$  term

Then we can check the hamiltonian of both Eq. ?? and Eq. ?? are time-reversal invariant:

$$\begin{aligned}
\hat{T}\hat{H}_0\hat{T}^{-1} &= \hat{T}\left[\sum_{i,\sigma}\varepsilon_{i,\sigma}a_{i,\sigma}^\dagger a_{i,\sigma} + \varepsilon_{i,\sigma}b_{i,\sigma}^\dagger b_{i,\sigma} + \sum_{\langle ij\rangle,\sigma}t_{ij}(a_{i,\sigma}^\dagger b_{j,\sigma} + h.c.)\right]\hat{T}^{-1} \\
&= \sum_{i,\sigma}\varepsilon_{i,\sigma}\hat{T}a_{i,\sigma}^\dagger a_{i,\sigma}\hat{T}^{-1} + \varepsilon_{i,\sigma}\hat{T}b_{i,\sigma}^\dagger b_{i,\sigma}\hat{T}^{-1} + \sum_{\langle ij\rangle,\sigma}t_{ij}^*(\hat{T}a_{i,\sigma}^\dagger b_{j,\sigma}\hat{T}^{-1} + h.c.) \\
&= \sum_{i,\sigma}\varepsilon_{i,\sigma}(-\sigma)^2a_{i,-\sigma}^\dagger a_{i,-\sigma} + \varepsilon_{i,\sigma}(-\sigma)^2b_{i,-\sigma}^\dagger b_{i,-\sigma} + \sum_{\langle ij\rangle,\sigma}t_{ij}^*((-\sigma)^2a_{i,-\sigma}^\dagger b_{j,-\sigma} + h.c.) \\
&= \sum_{i,\sigma}\varepsilon_{i,\sigma}a_{i,\sigma}^\dagger a_{i,\sigma} + \varepsilon_{i,\sigma}b_{i,\sigma}^\dagger b_{i,\sigma} + \sum_{\langle ij\rangle,\sigma}t_{ij}^*(a_{i,\sigma}^\dagger b_{j,\sigma} + h.c.) = \hat{H}_0
\end{aligned}$$

, if the condition is satisfied:  $t_{ij}^* = t_{ij}$ .

$$\begin{aligned}
\hat{T}\hat{H}_0\hat{T}^{-1} &= \hat{T}\left[\sum_{\mathbf{k},\sigma}\begin{pmatrix} a_{\mathbf{k},\sigma}^\dagger & b_{\mathbf{k},\sigma}^\dagger \end{pmatrix} \begin{pmatrix} H_{AA} & H_{AB} \\ H_{BA} & H_{BB} \end{pmatrix} \begin{pmatrix} a_{\mathbf{k},\sigma} \\ b_{\mathbf{k},\sigma} \end{pmatrix}\right]\hat{T}^{-1} \\
&= \left[\sum_{\mathbf{k},\sigma}\begin{pmatrix} (-\sigma)a_{-\mathbf{k},-\sigma}^\dagger & (-\sigma)b_{-\mathbf{k},-\sigma}^\dagger \end{pmatrix} \hat{T} \begin{pmatrix} H_1(k) & 0 \\ 0 & H_1^*(-k) \end{pmatrix} \hat{T}^{-1} \begin{pmatrix} (-\sigma)a_{-\mathbf{k},-\sigma} \\ (-\sigma)b_{-\mathbf{k},-\sigma} \end{pmatrix}\right] \\
&= \left[\sum_{\mathbf{k},\sigma}\begin{pmatrix} (-\sigma)a_{-\mathbf{k},-\sigma}^\dagger & (-\sigma)b_{-\mathbf{k},-\sigma}^\dagger \end{pmatrix} \begin{pmatrix} H_1(-k) & 0 \\ 0 & H_1^*(k) \end{pmatrix} \begin{pmatrix} (-\sigma)a_{-\mathbf{k},-\sigma} \\ (-\sigma)b_{-\mathbf{k},-\sigma} \end{pmatrix}\right] \\
&= \left[\sum_{\mathbf{k},\sigma}\begin{pmatrix} (-\sigma)a_{-\mathbf{k},-\sigma}^\dagger & (-\sigma)b_{-\mathbf{k},-\sigma}^\dagger \end{pmatrix} \begin{pmatrix} H_1(-k) & 0 \\ 0 & H_1^*(k) \end{pmatrix} \begin{pmatrix} (-\sigma)a_{-\mathbf{k},-\sigma} \\ (-\sigma)b_{-\mathbf{k},-\sigma} \end{pmatrix}\right] \\
&= \left[\sum_{\mathbf{k},\sigma}\begin{pmatrix} a_{-\mathbf{k},-\sigma}^\dagger & b_{-\mathbf{k},-\sigma}^\dagger \end{pmatrix} \begin{pmatrix} H_1(-k) & 0 \\ 0 & H_1^*(k) \end{pmatrix} \begin{pmatrix} a_{-\mathbf{k},-\sigma} \\ b_{-\mathbf{k},-\sigma} \end{pmatrix}\right] = \hat{H}_0
\end{aligned}$$

where  $T$  only has complex operation on matrix elements because the  $2 \times 2$  matrix  $H(\mathbf{k}) = \begin{pmatrix} H_{AA} & H_{AB} \\ H_{BA} & H_{BB} \end{pmatrix}$  is expressed in pseudospin space (by  $\tau$ ) not the spin space.

Please note that, under the time-reversal transformation, the total hamiltonian  $\hat{H}_0$  is invariant, but the cornel  $H(\mathbf{k}) = \begin{pmatrix} H_{AA} & H_{AB} \\ H_{BA} & H_{BB} \end{pmatrix}$  is NOT. Generally, the cornel hamiltonian is transferred like:  $TH(\mathbf{k})T^{-1} = H(-\mathbf{k})$ , which shows the momentum  $\mathbf{k}$  is mapped to its time-reversal partner  $-\mathbf{k}$ . Here  $H(\mathbf{k})$  and  $T$  are both matrix form, thus in many literatures people only discuss how the cornel hamiltonian  $H(\mathbf{k})$  transforms instead of the whole hamiltonian operator  $\hat{H}_0$  !!

## 2. Inversion symmetry with $t_1$ term

Then we can check the hamiltonian of  $H_0$  are inversional invariant:

$$\begin{aligned}
\hat{I}\hat{H}_0\hat{I}^{-1} &= \hat{I}\left[\sum_{i,\sigma}\varepsilon_{i,\sigma}a_{i,\sigma}^\dagger a_{i,\sigma} + \varepsilon_{i,\sigma}b_{i,\sigma}^\dagger b_{i,\sigma} + \sum_{\langle ij\rangle,\sigma}t_{ij}(a_{i,\sigma}^\dagger b_{j,\sigma} + h.c.)\right]\hat{I}^{-1} \\
&= \sum_{i,\sigma}\varepsilon_{i,\sigma}\hat{I}a_{i,\sigma}^\dagger a_{i,\sigma}\hat{I}^{-1} + \varepsilon_{i,\sigma}\hat{I}b_{i,\sigma}^\dagger b_{i,\sigma}\hat{I}^{-1} + \sum_{\langle ij\rangle,\sigma}t_{ij}(\hat{I}a_{i,\sigma}^\dagger b_{j,\sigma}\hat{I}^{-1} + h.c.) \\
&= \sum_{i,\sigma}\varepsilon_{i,\sigma}b_{-i,\sigma}^\dagger b_{-i,\sigma} + \varepsilon_{i,\sigma}a_{-i,\sigma}^\dagger a_{-i,\sigma} + \sum_{\langle ij\rangle,\sigma}t_{ij}(b_{-i,\sigma}^\dagger a_{-j,\sigma} + h.c.) \\
&= \sum_{i,\sigma}\varepsilon_{-i,\sigma}b_{i,\sigma}^\dagger b_{i,\sigma} + \varepsilon_{-i,\sigma}a_{i,\sigma}^\dagger a_{i,\sigma} + \sum_{\langle ij\rangle,\sigma}t_{-i,-j}(b_{i,\sigma}^\dagger a_{j,\sigma} + h.c.) = \hat{H}_0
\end{aligned}$$

, if the conditions are satisfied:  $\varepsilon_{-i,\sigma} = \varepsilon_{i,\sigma}$  and  $t_{i,j} = t_{-j,-i}^*$ .

In momentum space,

$$\begin{aligned}
\hat{I}\hat{H}_0\hat{I}^{-1} &= \hat{I}\left[\sum_{\mathbf{k},\sigma}\begin{pmatrix} a_{\mathbf{k},\sigma}^\dagger & b_{\mathbf{k},\sigma}^\dagger \end{pmatrix} \begin{pmatrix} H_{AA} & H_{AB} \\ H_{BA} & H_{BB} \end{pmatrix} \begin{pmatrix} a_{\mathbf{k},\sigma} \\ b_{\mathbf{k},\sigma} \end{pmatrix}\right]\hat{I}^{-1} \\
&= \left[\sum_{\mathbf{k},\sigma}\begin{pmatrix} b_{-\mathbf{k},\sigma}^\dagger & a_{-\mathbf{k},\sigma}^\dagger \end{pmatrix} \hat{I} \begin{pmatrix} H_{AA} & H_{AB} \\ H_{BA} & H_{BB} \end{pmatrix} \hat{I}^{-1} \begin{pmatrix} b_{-\mathbf{k},\sigma} \\ a_{-\mathbf{k},\sigma} \end{pmatrix}\right] \\
&= \left[\sum_{\mathbf{k},\sigma}\begin{pmatrix} b_{-\mathbf{k},\sigma}^\dagger & a_{-\mathbf{k},\sigma}^\dagger \end{pmatrix} \begin{pmatrix} H_{AA}(\mathbf{k}) & H_{AB}(\mathbf{k}) \\ H_{BA}(\mathbf{k}) & H_{BB}(\mathbf{k}) \end{pmatrix} \begin{pmatrix} b_{-\mathbf{k},\sigma} \\ a_{-\mathbf{k},\sigma} \end{pmatrix}\right] \\
&= \left[\sum_{\mathbf{k},\sigma}\begin{pmatrix} b_{-\mathbf{k},\sigma}^\dagger & a_{-\mathbf{k},\sigma}^\dagger \end{pmatrix} [d_1(\mathbf{k})\tau_x + d_2(\mathbf{k})\tau_y + \varepsilon\tau_0 + \bar{\varepsilon}\tau_z] \begin{pmatrix} b_{-\mathbf{k},\sigma} \\ a_{-\mathbf{k},\sigma} \end{pmatrix}\right] \\
&= \left[\sum_{\mathbf{k},\sigma}\begin{pmatrix} b_{\mathbf{k},\sigma}^\dagger & a_{\mathbf{k},\sigma}^\dagger \end{pmatrix} [d_1(-\mathbf{k})\tau_x + d_2(-\mathbf{k})\tau_y + \varepsilon\tau_0 + \bar{\varepsilon}\tau_z] \begin{pmatrix} b_{\mathbf{k},\sigma} \\ a_{\mathbf{k},\sigma} \end{pmatrix}\right] \\
&= \left[\sum_{\mathbf{k},\sigma}\begin{pmatrix} a_{\mathbf{k},\sigma}^\dagger & b_{\mathbf{k},\sigma}^\dagger \end{pmatrix} [d_1(\mathbf{k})\tau_x + d_2(\mathbf{k})\tau_y + \varepsilon\tau_0 - \bar{\varepsilon}\tau_z] \begin{pmatrix} a_{\mathbf{k},\sigma} \\ b_{\mathbf{k},\sigma} \end{pmatrix}\right] \\
&= \hat{H}_0
\end{aligned}$$

, if and only if  $\bar{\varepsilon} = 0$  !! Please note that  $I$  doesnot change matrix elements because we put all operations on operators. Here we used the the quantity  $d_1(-x, -y) = d_1(x, y)$  and  $d_2(-x, -y) = -d_2(x, y)$ .



An alternative way is,

$$\begin{aligned}
\hat{I}\hat{H}_0\hat{I}^{-1} &= \hat{I}\left[\sum_{\mathbf{k},\sigma}\left(a_{\mathbf{k},\sigma}^\dagger, b_{\mathbf{k},\sigma}^\dagger\right)\begin{pmatrix} H_{AA} & H_{AB} \\ H_{BA} & H_{BB} \end{pmatrix}\begin{pmatrix} a_{\mathbf{k},\sigma} \\ b_{\mathbf{k},\sigma} \end{pmatrix}\right]\hat{I}^{-1} \\
&= \left[\sum_{\mathbf{k},\sigma}\left(a_{\mathbf{k},\sigma}^\dagger, b_{\mathbf{k},\sigma}^\dagger\right)\hat{I}\begin{pmatrix} H_{AA} & H_{AB} \\ H_{BA} & H_{BB} \end{pmatrix}\hat{I}^{-1}\begin{pmatrix} a_{\mathbf{k},\sigma} \\ b_{\mathbf{k},\sigma} \end{pmatrix}\right] \\
&= \left[\sum_{\mathbf{k},\sigma}\left(a_{\mathbf{k},\sigma}^\dagger, b_{\mathbf{k},\sigma}^\dagger\right)\tau_x[d_1(-\mathbf{k})\tau_x + d_2(-\mathbf{k})\tau_y + \varepsilon\tau_0 + \bar{\varepsilon}\tau_z]\tau_x\begin{pmatrix} a_{\mathbf{k},\sigma} \\ b_{\mathbf{k},\sigma} \end{pmatrix}\right] \\
&= \left[\sum_{\mathbf{k},\sigma}\left(a_{\mathbf{k},\sigma}^\dagger, b_{\mathbf{k},\sigma}^\dagger\right)[d_1(-\mathbf{k})\tau_x - d_2(-\mathbf{k})\tau_y + \varepsilon\tau_0 - \bar{\varepsilon}\tau_z]\begin{pmatrix} a_{\mathbf{k},\sigma} \\ b_{\mathbf{k},\sigma} \end{pmatrix}\right] \\
&= \left[\sum_{\mathbf{k},\sigma}\left(a_{\mathbf{k},\sigma}^\dagger, b_{\mathbf{k},\sigma}^\dagger\right)[d_1(\mathbf{k})\tau_x + d_2(\mathbf{k})\tau_y + \varepsilon\tau_0 - \bar{\varepsilon}\tau_z]\begin{pmatrix} a_{\mathbf{k},\sigma} \\ b_{\mathbf{k},\sigma} \end{pmatrix}\right] \\
&= \hat{H}_0
\end{aligned}$$

, where we put operation on the hamiltonian cornel, that is  $I\begin{pmatrix} H_{AA}(\mathbf{k}) & H_{AB}(\mathbf{k}) \\ H_{BA}(\mathbf{k}) & H_{BB}(\mathbf{k}) \end{pmatrix}\hat{I}^{-1} = \tau_x\begin{pmatrix} H_{AA}(-\mathbf{k}) & H_{AB}(-\mathbf{k}) \\ H_{BA}(-\mathbf{k}) & H_{BB}(-\mathbf{k}) \end{pmatrix}\tau_x$ . The operation of  $I = \tau_x\bar{K}$ , where  $\tau_x$  exchanges sublattice and  $\bar{K}$  inverse momentum  $\mathbf{k}$  to  $-\mathbf{k}$ .

### 3. Symmetries with flux terms

Haldane model is an extension of graphene honeycomb lattice. Except for the nearest neighbor (NN) hopping, Haldane added the next nearest neighbor (NNN) hopping in honeycomb lattice. In particular, the NNN hopping carries a phase  $t_2e^{\pm i\phi}$ , the  $\pm$  depends on the arrow as shown in Fig.

We write the additional term as

$$H_{\text{haldane}} = \sum_{\langle\langle ij \rangle\rangle} e^{i\nu_{ij}\phi} a_{i,\sigma}^\dagger a_{j,\sigma} + \nu_{ij} b_{i,\sigma}^\dagger b_{j,\sigma} \quad (115)$$

, where  $\nu_{ij} = \pm 1$  follows the direction of hoppings and we assume both spin up and down take the same hopping signs.

In the  $\mathbf{k}$ -representation, Hamiltonian are:

$$H_{\text{haldane}} = \sum_{\mathbf{k}, \sigma} d_{15}(\mathbf{k}) a_{\mathbf{k}, \sigma}^\dagger a_{\mathbf{k}, \sigma} - d_{15}(\mathbf{k}) b_{\mathbf{k}, \sigma}^\dagger b_{\mathbf{k}, \sigma} \quad (116)$$

where

$$d_{15} = 2t_2 \sin \phi \sum_i \sin \mathbf{k} \cdot \mathbf{b}_i$$

Let us check the symmetry of Haldane model. For time-reversal symmetry, we have

$$\begin{aligned} \hat{T} H_{\text{haldane}} \hat{T}^{-1} &= \hat{T} \left[ \sum_{\langle\langle ij \rangle\rangle, \sigma} e^{i\nu_{ij}\phi} a_{i, \sigma}^\dagger a_{j, \sigma} + e^{i\nu_{ij}\phi} b_{i, \sigma}^\dagger b_{j, \sigma} \right] \hat{T}^{-1} \\ &= \sum_{\langle\langle ij \rangle\rangle, \sigma} e^{-i\nu_{ij}\phi} a_{i, -\sigma}^\dagger a_{j, -\sigma} + e^{-i\nu_{ij}\phi} b_{i, -\sigma}^\dagger b_{j, -\sigma} \\ &\neq H_{\text{haldane}} \end{aligned}$$

, which is NOT invariant, or time-reversal symmetry is explicitly breaking.

For inverse symmetry, we have

$$\begin{aligned} \hat{I} H_{\text{haldane}} \hat{I}^{-1} &= \hat{I} \left[ \sum_{\langle\langle ij \rangle\rangle, \sigma} e^{i\nu_{ij}\phi} a_{i, \sigma}^\dagger a_{j, \sigma} + e^{i\nu_{ij}\phi} b_{i, \sigma}^\dagger b_{j, \sigma} \right] \hat{I}^{-1} \\ &= \sum_{\langle\langle ij \rangle\rangle, \sigma} e^{i\nu_{ij}\phi} b_{-i, \sigma}^\dagger b_{-j, \sigma} + e^{i\nu_{ij}\phi} a_{-i, \sigma}^\dagger a_{-j, \sigma} \\ &= H_{\text{haldane}} \end{aligned}$$

where  $\nu_{-i, -j} = \nu_{ij}$ . So the inverse symmetry is preserved.

To check the symmetry operation in momentum space is straight-forward, similar to the previous section. For time-reversal symmetry,  $\hat{T} H_{\text{haldane}} \hat{T}^{-1} = H^*(\mathbf{k}) = H(\mathbf{k}) \neq H(-\mathbf{k})$ . For inverse symmetry,  $\hat{I} H_{\text{haldane}} \hat{I}^{-1} = \tau_x H(-\mathbf{k}) \tau_x = \tau_x d_{15}(-\mathbf{k}) \tau_z \tau_x = d_{15}(\mathbf{k}) \tau_z = H_{\text{haldane}}$ .

Following Haldane[? ], we introduce a second neighbor tight binding model on honeycomb lattice[? ],

$$\mathcal{H}_{SO} = \sum_{\langle\langle ij \rangle\rangle_{\alpha\beta}} i\lambda_{SO} \nu_{ij} s_{\alpha\beta}^z c_{i\alpha}^\dagger c_{j\beta}. \quad (117)$$

which connects second neighbors with a spin dependent amplitude.  $\nu_{ij} = -\nu_{ji} = \pm 1$ , depending on the orientation of the two nearest neighbor bonds  $\mathbf{d}_1$  and  $\mathbf{d}_2$  the electron traverses in going from site  $j$  to  $i$ .  $\nu_{ij} = \pm 1$  if the electron makes a left (right) turn to get to the second bond. The spin dependent term can be written in a coordinate independent representation as  $i(\mathbf{d}_1 \times \mathbf{d}_2) \cdot \mathbf{s}$ . Thus, the model is just two copies of Haldane model, with

spin up and spin down hosting conjugated hoppings, which should preserve time-reversal symmetry in global.

In the  $\mathbf{k}$ -representation, Hamiltonian are:

$$H_{Kane} = \sum_{\mathbf{k}, \sigma} s_z (d_{15}(\mathbf{k}) a_{\mathbf{k}, \sigma}^\dagger a_{\mathbf{k}, \sigma} - d_{15}(\mathbf{k}) b_{\mathbf{k}, \sigma}^\dagger b_{\mathbf{k}, \sigma}) \quad (118)$$

Let us check the symmetry of Kane-Mele model. For time-reversal symmetry, we have

$$\begin{aligned} \hat{T} H_{Kane} \hat{T}^{-1} &= \hat{T} [i\lambda_{SO} \sum_{\langle\langle ij \rangle\rangle, \sigma} s_z \nu_{ij} a_{i, \sigma}^\dagger a_{j, \sigma} + s_z \nu_{ij} b_{i, \sigma}^\dagger b_{j, \sigma}] \hat{T}^{-1} \\ &= -i\lambda_{SO} \sum_{\langle\langle ij \rangle\rangle, \sigma} (-s_z) \nu_{ij} a_{i, -\sigma}^\dagger a_{j, -\sigma} + (-s_z) \nu_{ij} b_{i, -\sigma}^\dagger b_{j, -\sigma} \\ &= H_{Kane} \end{aligned}$$

, which is time-reversal invariant.

For inverse symmetry, we have

$$\begin{aligned} \hat{I} H_{Kane} \hat{I}^{-1} &= \hat{I} [i\lambda_{SO} \sum_{\langle\langle ij \rangle\rangle, \sigma} s_z \nu_{ij} a_{i, \sigma}^\dagger a_{j, \sigma} + s_z \nu_{ij} b_{i, \sigma}^\dagger b_{j, \sigma}] \hat{I}^{-1} \\ &= i\lambda_{SO} \sum_{\langle\langle ij \rangle\rangle, \sigma} s_z \nu_{ij} b_{-i, \sigma}^\dagger b_{-j, \sigma} + s_z \nu_{ij} a_{-i, \sigma}^\dagger a_{-j, \sigma} \\ &= H_{Kane} \end{aligned}$$

where  $\nu_{-i, -j} = \nu_{ij}$ . So the inverse symmetry is preserved.

To check the symmetry operation in momentum space is straight-forward, similar to the previous section. For time-reversal symmetry,  $\hat{T} H_{Kane} \hat{T}^{-1} = i s_y [d_{15}(\mathbf{k}) \tau_z s_z] (-i s_y) = -d_{15}(\mathbf{k}) \tau_z s_z = H_{Kane}(-\mathbf{k})$ . For inverse symmetry,  $\hat{I} H_{Kane} \hat{I}^{-1} = \tau_x H(-\mathbf{k}) \tau_x = \tau_x d_{15}(-\mathbf{k}) \tau_z s_z \tau_x = d_{15}(\mathbf{k}) \tau_z s_z = H_{Kane}$ .

## $Z_2$ invariant

We have so far established that a new phase of matter exists in TR-invariant insulators, at least in two dimensions. The physical imprint of the state is the presence of gapless counterpropagating edge modes on each edge of a sample. These modes are protected from opening a gap by TR invariance if and only if there exist an odd number of pairs of them. That is, an even number of edge-state pairs are not protected from opening a gap. The edge-mode discussion suggests that there is a  $Z_2$ -type order in the QSH state. We will prove that

there exists a  $Z_2$  topological invariant and that there is a topological classification of QSH insulators (2-D insulators) with two different phases, between which we cannot go without closing the bulk gap.

*The bulkboundary correspondence:  $Z_2$  invariant from the bulk*

Consider the up-spin number current  $I^\uparrow$ , i.e., the current omitting the charge factor  $e$ . If we omit altogether the spin-flip terms, the model is a sum of two independent Haldane models with opposite fluxes for the two spin species. Therefore we have:

$$I^\uparrow = \frac{eV}{h} \quad (119)$$

due to an unbalance between the left-edge modes, and the right-edge ones, as previously discussed. A similar unbalance occurs for the down-spin number current, which has however opposite sign:

$$I^\downarrow = -\frac{eV}{h} \quad (120)$$

The two currents cancel, if you look at the total charge current  $I^{charge} = I^\uparrow + I^\downarrow = 0$ . But if you de

fine the spin current  $I^{spin} = \frac{1}{2}[I^\uparrow - I^\downarrow] = \frac{eV}{h}$ . The spin-conductivity is  $\sigma_{xy}^s = 1e^2/h$ . It is important to stress that the spin-current is quantized in terms of the spin given above correct when we neglect the spin-flip terms due to the Rashba spin-orbit coupling, and higher order spin-orbit induced spin-flip terms.

Next we check the possible band structure of QSHE in the presence of boundary, as shown in Fig. 11. Fig. (a) shows a sketch of 4 edge state bands in the bulk gap, two of them totally within the gap, two other only partially so. The solid circles correspond to TRIM. Each band has a time-reversal partner that we have denoted with different colors: a blue band is the Kramers degeneracy partner of a red band. Notice how red and blue bands (Kramers partners) join at the TRIM points, where the degeneracy occurs at the same  $k$  point. Although we have plotted edge states here, the situation depicted is rather that of a trivial insulator. Indeed, depending on the number of electrons in the system, and on the detailed shape of the bands, the Fermi energy might cut the bands in 2 points in the interval  $[0, \pi]$ . Consider now Fig. 11(b), showing a similar sketch of edge states in the bulk

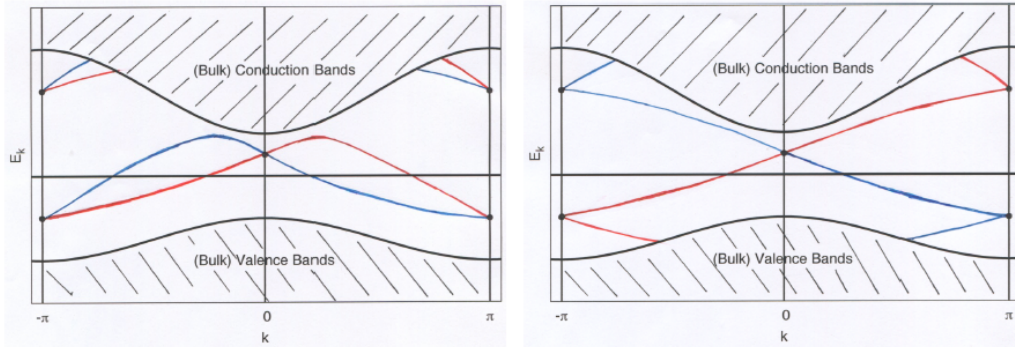


FIG. 11: The edge states for  $Z_2 = 0$  (left) and  $Z_2 = 1$  right plotted between  $\Gamma_a = 0$  and  $\Gamma_b = \pi/2$ , only half the BZ is shown because T requires it to be symmetric around  $k = 0$ . On the left the insulator is topologically trivial: the Fermi energy cuts the bands into 2 points in the interval  $[0, \pi/a]$ , but a modification of the bands could change that integer to 0 or to 4. On the right, the insulator is topologically non-trivial: the Fermi energy cuts the edge bands into 1 point in the interval  $[0, \pi/a]$  and there is no way we can change that into an even integer by deforming the bands.

gap: notice that the energy eigenvalues at the TRIM points are identical to those of Fig. 11(a), and again every red band has a inversion-partner blue band. Although these two edge state branches cross, this crossing will not turn into an anticrossing: the states cannot scatter into each other since they are on different layers. The two edge state branches are linked by time-reversal: they occupy the same position, but describe propagation in opposite directions.

At last of this section, we elucidate the importance of  $Z_2$  and time-reversal symmetry on the topological insulator. Let us consider a single pair of edge states, as shown in Fig. 11(b). Here our spin up electron has  $C = 1$ , so it has one left moving edge states  $v_F k$ . Spin down electrons have  $C = -1$ , so the edge states for spin down electrons are right moving  $-v_F k$ . We can write them together in one Hamiltonian as a  $2 \times 2$  matrix (in spin space space):

$$H_{edge} = \begin{pmatrix} v_F k & 0 \\ 0 & -v_F k \end{pmatrix} \quad (121)$$

Can one add any extra term to open a gap for the edge states? If we can open the gap for the edge states, we can move the chemical potential into the gap and the edge states turns into an insulator, as shown the case in Fig. 11(a). But if we can prove that no matter what

we do, we can NOT open a gap, the edge is always metallic, so we have a topologically protected edge state (topological insulator). The answer is No, if we preserve the time-reversal symmetry. (Yes, if we break the time-reversal symmetry.) To see it, for example, we add a mass term  $m\sigma_x$ , which breaks time-reversal symmetry:  $Tm\sigma_xT^{-1} = -m\sigma_x$ . This will open a gap in edge spectral and turns the topological insulator to a trivial insulator.

Assume the spin up state is in a quantum Hall state with  $C = 2$ , and the spin down state has  $C = -2$ . We will have two left moving electrons with spin up, and two right moving electrons with spin down.

$$\hat{H} = \sum_k \left( c_{k\uparrow}^\dagger, d_{k\uparrow}^\dagger, c_{k,\downarrow}^\dagger, c_{k,\downarrow}^\dagger \right) \begin{pmatrix} v_F k & 0 & 0 & 0 \\ 0 & v_F k & 0 & 0 \\ 0 & 0 & -v_F k & 0 \\ 0 & 0 & 0 & -v_F k \end{pmatrix} \begin{pmatrix} c_{k\uparrow} \\ d_{k,\uparrow} \\ c_{k,\downarrow} \\ c_{k,\downarrow} \end{pmatrix} \quad (122)$$

Now, one can add one extra term

$$\hat{H} = \sum_k \left( c_{k\uparrow}^\dagger, d_{k\uparrow}^\dagger, c_{k,\downarrow}^\dagger, c_{k,\downarrow}^\dagger \right) \begin{pmatrix} 0 & 0 & 0 & m \\ 0 & 0 & -m & 0 \\ 0 & -m & 0 & 0 \\ m & 0 & 0 & 0 \end{pmatrix} \begin{pmatrix} c_{k\uparrow} \\ d_{k,\uparrow} \\ c_{k,\downarrow} \\ c_{k,\downarrow} \end{pmatrix} \quad (123)$$

This Hamiltonian is time-reversally invariant by the time-reversal operator

$$T = \begin{pmatrix} 0 & 0 & 1 & 0 \\ 0 & 0 & 0 & 1 \\ -1 & 0 & 0 & 0 \\ 0 & -1 & 0 & 0 \end{pmatrix} K \quad (124)$$

It can be easily checked that the (k) we wrote above is invariant under time-reversal. However, the eigenvalue becomes  $E = \pm\sqrt{m^2 + v_F^2 k^2}$ , opening a gap in the edge spectra.

Thus, in a time-reversal invariant 2D system: the odd number of edge pairs is protected, but the even number is not. Thus we emphasize the  $Z_2$  number in TI.

### *$Z_2$ Invariant as Zeros of the Pfaffian*

We would like to obtain an index whose behavior tells us about whether the system is a topological insulator or not. But this process is more complicated than the Chern number.

There are many different (but equivalent) ways to do so, which will not be discussed in the lecture because it is too technical.

A simple introduction is, since we know our index must contain the time-reversal operator, it is intuitive to consider the antisymmetric matrix of overlaps of the  $i$ -th eigenstate with the time reversal of the  $j$ -th eigenstate:

$$\langle u_i(k)|T|u_j(k)\rangle = (u_i^*(k))_m U_{mn} (u_j^*(k))_n = -(u_j^*(k))_n U_{nm} (u_i^*(k))_m = -\langle u_j(k)|T|u_i(k)\rangle \quad (125)$$

where  $T = UK$ , with  $U$  a unitary, antisymmetric matrix. For a  $2 \times 2$  matrix, we have

$$\langle u_i(k)|T|u_j(k)\rangle = \epsilon_{ij} P(k) = \begin{pmatrix} 0 & P(k) \\ -P(k) & 0 \end{pmatrix} \quad (126)$$

$$P(k) = \text{Pf}[\langle u_i(k)|T|u_j(k)\rangle] \quad (127)$$

where  $P(k)$  is the Pfaffian of the matrix. For a  $2 \times 2$  matrix, the Pfaffian picks the  $A_{12}$  component.

Pfaffian is useful, because the following fact. Let us consider the Hilbert space spanned by  $|u_1(k)\rangle$  and  $T|u_1(k)\rangle$  (they are orthogonal). In this case,  $\langle u_1(k)|T|u_1(k)\rangle = 0$ , but  $\langle u_1(k)|T|u_2(k)\rangle \neq 0$ . So we see  $|P(k)| = 1$  at T-invariant points, hence we set  $P(k) = e^{i\phi(k)}$ .

Can we make a smooth choice for the phase of all states such that  $P(k)$  never vanishes for all BZ? The answer is: yes if the insulator is topologically trivial, no if it is non-trivial. More in general, Kane and Mele argue that the number of zeroes that  $P(k)$  shows in half of the  $\text{BZ}_+$  so defined such that  $k$  and  $-k$  are never both contained – is a  $\mathbb{Z}_2$  invariant: even in the trivial case, odd in the non-trivial one, which can be calculated by the winding number of the phase of  $\log[P(k)]$  in complex plane, as  $k$  moves along a contour  $C$  around  $\text{BZ}_+$ :

$$I = \frac{1}{2\pi i} \int_C d\mathbf{k} \cdot \nabla \ln(P(\mathbf{k})) \quad (128)$$

TR symmetry identifies two important subspaces of the space of Bloch Hamiltonians  $H(k)$  and the corresponding occupied band wave functions  $|u_i(k)\rangle$ . The “even” subspace, for which  $TH(k)T^{-1} = H(k)$ , have the property that  $T|u_i(k)\rangle$  is equivalent to  $|u_i(k)\rangle$  up to a phase. So the TR symmetric points in BZ  $(0, 0, 0, \pi, \pi, 0, \pi, \pi)$  are belong to the even subspace. The odd subspace has wave functions with the property that the space spanned by  $T|u_i(k)\rangle$  is orthogonal to the space spanned by  $|u_i(k)\rangle$ . We will establish the  $\mathbb{Z}_2$  classification by studying the set of  $k$  which belong to the odd subspace.

We now claim that the zeros of the Pfaffian in half of the BZ are a topological invariant. First, the zeros of  $P(k)$  should appear in pair, due to the TR symmetry. That is, if a zero appears at  $k^*$ , there should be another zero at  $-k^*$ . Second, if no spatial symmetries constrain its form, the zeros of  $P(k)$  are found by tuning two parameters, and generically occur at points in the Brillouin zone. We cut the BZ in half, making sure that the points  $k^*$ ,  $-k^*$  belong to different halves of the BZ. Assume that in half the BZ, we have one zero of the Pfaffian. This zero has a vorticity and hence cannot disappear directly similar to the situation of the graphene Dirac node. The zeros of the Pfaffian can move toward a TR-invariant point (and that is the only place they could possibly annihilate if there is one zero in half the BZ), but it turns out that the zeros cannot annihilate. If they could, it would mean that we can have a zero of the Pfaffian exactly at the TR-invariant point. However, we have proved that the TR-invariant point belongs to the even subspace, which has Pfaffian of unit modulus. Hence, one Pfaffian zero in half the BZ is stable globally. Third, an even number of zeros, of any vorticity, can be annihilated without joining at a TR-invariant point. If we have two vortices of different vorticity in half a BZ, they can always meet up and annihilate. If they have identical vorticity signs, they can meet up with the zeros in the other half of the BZ and annihilate because in this case they do not need to meet up at a TR-invariant point. An odd number of zeros can again annihilate two by two until the very last one.

We now show the explicit case of the Pfaffian invariant in the Kane and Mele model. At the valley K point, the Hamiltonian has a  $U(1) \times U(1)$  conservation law and, we have

$$h_{\uparrow}(\mathbf{K}) = \begin{pmatrix} M + 3\sqrt{3}t_2 & 0 \\ 0 & -(M + 3\sqrt{3}t_2) \end{pmatrix} \quad (129)$$

$$h_{\downarrow}(\mathbf{K}) = \begin{pmatrix} M - 3\sqrt{3}t_2 & 0 \\ 0 & -(M - 3\sqrt{3}t_2) \end{pmatrix} \quad (130)$$

We again start looking at  $M \gg t_2$  limit, the occupied bands are

$$E_1 = -(M + 3\sqrt{3}t_2), \quad |\rangle = (0, 1, 0, 0)^T \quad (131)$$

$$E_2 = -(M - 3\sqrt{3}t_2), \quad |\rangle = (0, 0, 0, 1)^T \quad (132)$$



The T-matrix is

$$T = \begin{pmatrix} 0 & 0 & 1 & 0 \\ 0 & 0 & 0 & 1 \\ -1 & 0 & 0 & 0 \\ 0 & -1 & 0 & 0 \end{pmatrix} K \quad (133)$$

and then by direct computation  $\langle u_1(k)|T|u_2(k)\rangle = 1$ . Hence the Pfaffian is equal 1 at the point K. When M is small and in the topological phase, we have occupied bands are

$$E_1 = -(M + 3\sqrt{3}t_2), \quad |\rangle = (0, 1, 0, 0)^T \quad (134)$$

$$E_2 = (M - 3\sqrt{3}t_2), \quad |\rangle = (0, 0, 1, 0)^T \quad (135)$$

and then by direct computation  $\langle u_1(k)|T|u_2(k)\rangle = 0$ . Thus, we see the space spanned by  $u_i(K)$  is orthogonal to that spanned by  $T|u_i(K)\rangle$ . In this example, we clearly see, there is one zero in Pfaffian in the half BZ for non-trivial phase, however, there is not zero in the trivial phase. This definition of  $Z_2$  invariant can classify the topological phase. At the critical point, by time reversal, a level crossing at K is accompanied by a level crossing at K', but the key is to look at level crossings in only half of the BZ.

At the trivial phase, we have Pfaffian equals 1 and at the non-trivial phase the Pfaffian equals zero. There should be a level crossing in half of the BZ at the critical point, which changes the Pfaffian from 1 to 0. We have now just proved that a topological phase transition with change of Pfaffian from unity to zero happens through a Dirac mass gap changing sign in half the BZ. This behavior is generic. The appearance of a Pfaffian zero in half the BZ is directly related to the switching of a Dirac fermion mass. We can find zeros of  $P(k)$  by tuning  $k_x, k_y$ ; hence, if they exist they are generically isolated points in the BZ. If they do not exist, we are in a trivial phase. If  $C_3$  symmetry is present, the zeros of the Pfaffian can be only at the only  $C_3$  symmetric places in the BZ, which are the  $K, K'$  points.

#### *The $Z_2$ invariant for systems with inversion symmetry*

By its standard definition, inversion around the origin is  $r \leftrightarrow r$ . When we apply inversion to the wavefunction of a particle with spin, it should not change the spin, but should flip the momentum. If the particle has some other ‘‘pseudospin’’ degrees of freedom, the action

of inversion on these is represented by a unitary matrix  $P$ . Inversion should commute with time reversal.

$$P^\dagger P = 1 \quad (136)$$

$$P^2 = 1 \quad (137)$$

$$PH(k)P^{-1} = H(-k) \quad (138)$$

$$PT = TP \quad (139)$$

A concrete example for inversion symmetry is given by the BHZ model. It can be checked directly that this has inversion symmetry represented by  $P = \sigma_z \tau_0$ .

Consider the Time-Reversal Invariant Momenta (TRIM),  $\Gamma_j$ . There are  $2^d$  such momenta in a  $d$ -dimensional lattice model. Each eigenstate  $|\Psi\rangle$  at these momenta has an orthogonal Kramers pair  $T|\Psi\rangle$ . If  $H$  is inversion symmetric,  $|\Psi\rangle$  can be chosen to be an eigenstate of  $P$  as well, therefore, the Kramers pair has to have the same parity eigenvalue:

$$PT|\Psi\rangle = TP|\Psi\rangle = T(\pm)|\Psi\rangle = \pm T|\Psi\rangle \quad (140)$$

Therefore, in a system with both time-reversal and inversion symmetry, we get  $2^d$  topological invariants. These are the products of the parity eigenvalues  $\xi_m(\Gamma_j)$  of the occupied Kramers pairs at  $\Gamma_j$ , for  $j = 1, \dots, 2^d$ .

Without proof, we quote the statement, that the following product turns out to be the same as the  $Z_2$  invariant

$$(-)^D = \prod_j \prod_m \xi_m(\Gamma_j) \quad (141)$$

We can check the above construction for the BHZ model. At each TRIM, the Hamiltonian is proportional to the parity operator  $P = \sigma_z \tau_0$ .

$$H(k = (0, 0)) = (\Delta + 2)\sigma_z \tau_0 \quad (142)$$

$$H(k = (0, \pi)) = \Delta\sigma_z \tau_0 \quad (143)$$

$$H(k = (\pi, 0)) = (\Delta - 2)\sigma_z \tau_0 \quad (144)$$

$$H(k = (\pi, \pi)) = \Delta\sigma_z \tau_0 \quad (145)$$

If  $\Delta > 2$ , at all four TRIM, the occupied Kramers pair is the one with  $\sigma_z \tau_0$  eigenvalue of  $-1$ , so giving  $D = 0$ . Likewise, if  $\Delta < -2$ , the eigenvalues are all 1, and we again obtain

$D = 0$ . For  $0 < \Delta < 2$ , we have P eigenvalues  $-1, -1, 1, -1$  at the four TRIM, respectively, whereas if  $-2 < \Delta < 0$ , we have  $-1, 1, 1, 1$ . In both cases, we have  $D = 1$ .

### Comparison with IQHE

The time-reversal invariant 2D topological insulators are also known as the quantum spin Hall effect (QSHE).

Symmetry: IQHE: Must break the time-reversal symmetry. Otherwise there is no Hall effect. QSHE: Must preserve the time-reversal symmetry. Otherwise the edge states are not topologically protected.

Stability: IQHE: More stable. Once we have IQHE, as long as we don't close the gap, the edge state will always be there. QSHE: Less stable. If one breaks the time-reversal symmetry, the edge states can be killed.

Impurity scatterings IQHE: No impurity scatterings at all. QSHE: Impurities cannot reflect one electron, because it breaks the time-reversal symmetry. But impurities can reflect two-electrons simultaneously, which doesn't break the time-reversal symmetry. There are impurity scatterings, but it is weaker than an ordinary 1D wire

Experimental signature: IQHE: Quantized Hall conductivity (perfect quantization, error bar is small). QSHE: Conductivity  $2e^2/h$  (2 comes from the fact that we have two edge states). Notice that 1. this is conductivity NOT Hall conductivity. 2. this quantization is much less accurate (error bar for clear samples with very small size, very large deviation for larger samples or dirty samples). This is because the impurity scattering here is non-zero.

Interactions? If we ignore the interactions and consider free fermions, IQHE and QSHE has little difference (the latter is just two copies of the former). However, if we consider interacting fermions: IQHE: We know that all the effects remain the same in the presence of strong interactions (in addition to the free fermion band structure theory, we also have the gauge theory, Green's function theory, and flux insertion techniques, which tell us that the Hall conductivity will remain integer-valued, even if we have very strong interactions in our system). QSHE: We don't have full understanding about interactions: What is the gauge theory that describes (maybe BF theory)? Whether the conductivity is still  $2e^2/h$  in the presence of strong interactions?

3D IQHE: Can only happen in even dimensions 2, 4, 6 ... There is no IQHE in 3D.

QSHE: Can be generalized to 3D

### 3D topological insulators

Time-reversal invariant topological insulator can be generalized to 3D. 3D topological insulators are described by four  $Z_2$  topological indices. Three of them are known as weak topological indices and the last one is known as the strong topological index.

Consider the 3D BZ of a 3D insulator. Now, we consider constant  $k_z$  planes. We can consider each constant  $k_z$  plane as a 2D system. For most constant  $H(k_z)$  planes, they are not time-reversally invariant 2D systems, because  $k_z$  under time-reversal. However, the  $k_z = 0$  and  $k_z = \pi$  planes are time-reversally invariant, because  $k_z$  is the same as  $k_z$  at 0 and  $\pi$ .

Now we consider  $k_z = 0$  plane as a 2D time-reversal invariant insulator and  $k_z = \pi$  plane as another 2D time-reversal invariant insulator. We can ask whether these two 2D planes are topological insulators or trivial insulators. There are three possibilities: both trivial, both topological, one topological and one trivial. Case I: both are trivial: the 3D insulator is topologically trivial. Case II: both are nontrivial: the 3D insulator is a weak topological insulator. Case III: one is trivial and the other is topological: the 3D insulator is a strong topological insulator.

Weak topological insulators, one way to understand the weak topological insulator is: it is just a stack of 2D topological insulators (stacked along the z-axis). The edge is not stable as we mentioned before. Strong topological insulators is more stable.

## TOPOLOGICAL SEMIMETAL

The starting interests came from the remarkable discovery of topological insulators, but the focus has recently shifted towards topological semimetals and even metals. In this section we study symmetry-enforced band crossings that are not movable. These band crossings, which are required to exist by symmetry alone, exhibit the following properties:

- They are protected by nonsymmorphic crystal symmetries, possibly together with nonspatial symmetries. A nonsymmorphic symmetry is a symmetry  $G = g|t/n$ , which combines a point-group symmetry  $g$  with a translation  $t/n$  by a fraction of a Bravais lattice vector.
- Symmetry-enforced band crossings are characterized by a global topological charge, which measures the winding of the eigenvalue of  $G$  as we go through the BZ. One needs to go twice (or  $n$  times) through the BZ in order to get back to the same eigenvalue.
- Symmetry-enforced band crossings are globally stable. That is, they cannot be removed, even by large symmetry-preserving deformations. They are required to exist by symmetry alone, independent of any other material details (e.g, chemical composition or energetics of the bands).

### Nonsymmorphic symmetries enforced band crossings

Nonsymmorphic symmetries  $G = \{g|t/n\}$  combine a point-group symmetry  $g$  with a translation  $t$  by a fraction of a Bravais lattice vector. Applying an  $n$ -fold nonsymmorphic symmetry  $n$  times yields a translation  $G^n = \pm t$ . The sign on the right-hand side originates from  $g^n$ , which equals  $-1$  for spin-1/2 quasiparticles (Bloch electrons with spin-orbit coupling) and  $1$  for spinless quasiparticles (Bloch electrons without spin-orbit coupling).

Two simple examples of nonsymmorphic symmetries: 1) a glide reflection  $M = m|t/2$ , with  $M^2 = \pm t$ ; 2) a two-fold screw rotation  $C_2 = C_2|t/2$ , with  $(C_2)^2 = \pm t$ .

In the band structure of materials with nonsymmorphic symmetries, the operators  $G$  can enforce band degeneracies in the  $g$ -invariant space of the BZ, i.e., on lines or planes which satisfy  $G * k = k$ . In these  $G$ -invariant spaces, the Bloch states  $|u_m(k)\rangle$  can be constructed in such a way that they are simultaneous eigenfunctions of both  $G$  and the Hamiltonian. To

derive the G-eigenvalues of the Bloch states  $|u_m(k)\rangle$ , we observe that  $G^n = \pm e^{ika}$ . Because of the phase factor  $e^{ika/n}$  in the eigensectors of G can switch, as  $k$  moves along the g-invariant space. From this it follows that pairs of bands must cross at least once within the invariant space. With this we have found the basic mechanism that leads to symmetry-enforced band degeneracies.

### A toy model

Supposed that we have a one-dimensional two-band system, as shown in Fig. 12: We just focus on the symmetry analysis without going to the details of hamiltonian elements.

First, the system has a translational symmetry, as  $\hat{T}(a)$ :

$$\hat{T}(a)|\psi\rangle = t(a)|\psi\rangle = e^{ika}|\psi\rangle \quad (146)$$

Second, if the system host a glide symmetry  $\hat{G}$  as shown in Fig. 12, we have the relation:

$$\hat{G}|\psi\rangle = g|\psi\rangle \quad (147)$$

Since two consecutive operation of  $\hat{G}$  equivalent to one translational operation  $\hat{T}(a)$ , we have

$$\hat{G}^2 = \hat{T}(a), \Rightarrow g^2 = t(a) = e^{ika}, \Rightarrow g = \pm e^{i\frac{ka}{2}} \quad (148)$$

To reveal the essential role played by the symmetries, let us recall that glide symmetry

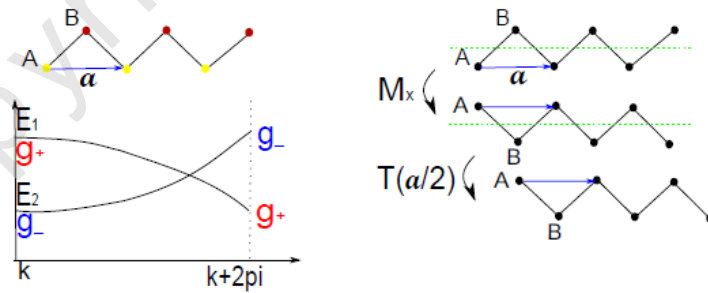


FIG. 12: A toy model with glide symmetry and cartoon picture about the band structure. The system has a translational symmetry expressed as  $\hat{T}(a)$ , where  $a$  is the lattice constant. Another symmetry is so-called glide symmetry as shown on the right, which is a combined symmetry with mirror operation  $M_x$  and translational operation by  $a/2$ .

commutes with hamitonian  $[\hat{G}, \hat{H}] = 0$ , which means that  $G(k)$  and  $H(k)$  can be simultaneously diagonalized by the same set of eigenstates:

$$H(k)|\psi_{\pm}(k)\rangle = E(k)|\psi_{\pm}(k)\rangle, \quad G(k)|\psi_{\pm}(k)\rangle = g_{\pm}(k)|\psi_{\pm}(k)\rangle \quad (149)$$

Generally speaking, at momentum  $k$ , we have two energy band  $E_1(k)$  and  $E_2(k)$ . Due to the periodic property of Brillium zone, we know  $E_{1(2)}(k + 2\pi) = E_{1(2)}(k)$ . However, we have

$$g_+(k + 2\pi) = -e^{i\frac{k\alpha}{2}} = g_-(k), \quad g_-(k + 2\pi) = e^{i\frac{k\alpha}{2}} = g_+(k) \quad (150)$$

Therefore, the two bands must cross each other when  $k$  changes by  $2\pi$  !

### A spinless model in one-dimension

Simply double unit cell of one-dimensional chain is one of this case. See SSH model.

### A spinful model in one-dimension

Here we propose a one-dimension spinful hamiltonian with two sublattices:

$$\begin{aligned} \hat{H} &= \hat{H}_0 + \hat{H}_1 \\ \hat{H}_0 &= t_0 \sum_{\langle ij \rangle, \sigma} (a_{i,\sigma}^\dagger b_{i,\sigma} + b_{i,\sigma}^\dagger a_{i+1,\sigma} + h.c.) \\ \hat{H}_1 &= t_1 \sum_{\langle ij \rangle} e^{-i\phi} a_{i,\uparrow}^\dagger b_{i,\downarrow} - e^{i\phi} a_{i,\downarrow}^\dagger b_{i,\uparrow} - e^{i\phi} b_{i,\uparrow}^\dagger a_{i+1,\downarrow} + e^{-i\phi} b_{i,\downarrow}^\dagger a_{i+1,\uparrow} + h.c. \end{aligned} \quad (151)$$

,where  $a_\sigma^\dagger$  and  $b_\sigma^\dagger$  creates one electron on sublattice A and B. In the momentum space,

$$\hat{H} = \sum_{\mathbf{k}} (a_{\mathbf{k},\uparrow}^\dagger, b_{\mathbf{k},\uparrow}^\dagger, a_{\mathbf{k},\downarrow}^\dagger, b_{\mathbf{k},\downarrow}^\dagger) \begin{pmatrix} 0 & \gamma(k) & 0 & \alpha(k) \\ \gamma(k) & 0 & -\beta(k) & 0 \\ 0 & -\beta(k) & 0 & \gamma(k) \\ \alpha(k) & 0 & \gamma(k) & 0 \end{pmatrix} \begin{pmatrix} a_{\mathbf{k},\uparrow} \\ b_{\mathbf{k},\uparrow} \\ a_{\mathbf{k},\downarrow} \\ b_{\mathbf{k},\downarrow} \end{pmatrix} \quad (152)$$

where  $\alpha(k) = 2t_1 \cos(\frac{k}{2} + \phi)$  and  $\beta(k) = \alpha(-k)$ ,  $\gamma(k) = 2t_0 \cos(\frac{k}{2})$ .

The current hamiltonian satisfies time-reversal symmetry and glide symmetry. That is,

$$\hat{T} : (a_{i,\sigma}^\dagger, b_{i,\sigma}^\dagger) \rightarrow (-\sigma a_{i,-\sigma}^\dagger, -\sigma b_{i,-\sigma}^\dagger), \text{ or } (a_{k,\sigma}^\dagger, b_{k,\sigma}^\dagger) \rightarrow (-\sigma a_{-k,-\sigma}^\dagger, -\sigma b_{-k,-\sigma}^\dagger), \quad \Theta = i s_y K \quad (153)$$

and

$$\hat{G} : (a_{i,\sigma}^\dagger, b_{i,\sigma}^\dagger) \rightarrow -i(b_{i,-\sigma}^\dagger, a_{i+1,-\sigma}^\dagger), \text{ or } (a_{k,\sigma}^\dagger, b_{k,\sigma}^\dagger) \rightarrow -ie^{-i\frac{k}{2}}(b_{k,-\sigma}^\dagger, a_{k,-\sigma}^\dagger), \quad \mathcal{G} = -i\tau_x s_x e^{-i\frac{k}{2}} \quad (154)$$

, where  $\Theta$  and  $\mathcal{G}$  are related operator representations.

The symmetry analysis is as follows. Time-reversal symmetry

$$\hat{T}\hat{H}\hat{T}^{-1} = \hat{H} \Leftarrow \Theta H(k)\Theta^{-1} = H(-k) \quad (155)$$

and glide symmetry

$$\hat{G}\hat{H}\hat{G}^{-1} = \hat{H} \Leftarrow \mathcal{G}H(k)\mathcal{G}^{-1} = H(k) \quad (156)$$

However,

$$\Theta\mathcal{G}(k)\Theta^{-1} = is_y K[-i\tau_x s_x e^{-ik/2}]K(-is_y) = -i\tau_x s_x e^{ik/2} = \mathcal{G}(-k) \quad (157)$$

To understand the connection, we need consider the eigenvalues of a Kramer pair at high-symmetry point, i.e.  $u(k)$  and  $Tu(k) = u^*(-k) = u^*(k)$  [please note  $u(k)$  and  $u^*(k)$  are orthogonal to each other]. Suppose that

$$\mathcal{G}(k=0)u(k=0) = iu(k=0), \quad (158)$$

where the eigenvalue is from  $\mathcal{G}^2(k=0) = (-i\tau_x s_x)^2 = -1$ . Then we have

$$\mathcal{G}(k=0)u^*(k=0) = \mathcal{G}(k=0)Tu(k=0) = T\mathcal{G}(k=0)u(k=0) = Tiu(k=0) = -iTu(k=0) = -iu^*(k=0) \quad (159)$$

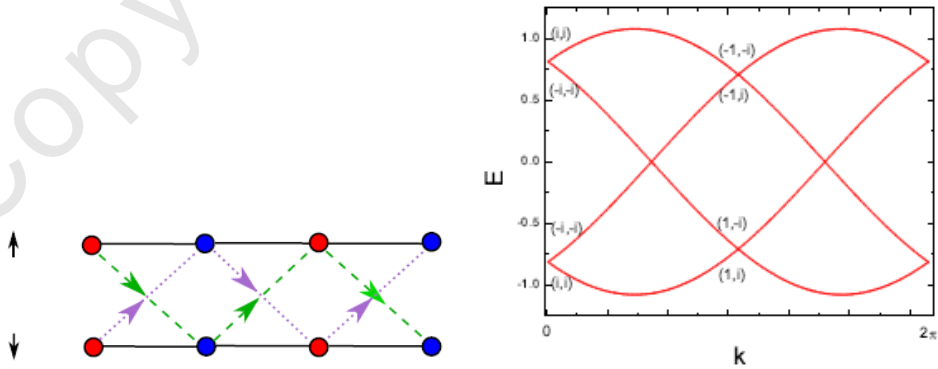


FIG. 13: A one-dimensional spinful model with glide symmetry. Each unit cell encloses two sublattice ( $A(B)$ ) and two spins  $\uparrow(\downarrow)$ .



Thus we have for the Kramer pair at  $k = 0$ , they have opposite eigenvalues in operator  $\mathcal{G}(k = 0)$ .

Similarly, we can know, at momentum  $k = \pi$ , Kramer pair have the same eigenvalues in operator  $\mathcal{G}(k = \pi)$ , since  $\mathcal{G}(k = \pi)^2 = 1$ :

$$\mathcal{G}(k = \pi)u(k = \pi) = u(k = \pi), \quad (160)$$

$$\mathcal{G}(k = \pi)u^*(k = \pi) = \mathcal{G}(k = \pi)Tu(k = \pi) = T\mathcal{G}(k = \pi)u(k = \pi) = Tu(k = \pi) = u^*(k = \pi) \quad (161)$$

At last, we discuss the connection between  $k = 0$  and  $k = \pi$ . Since  $\mathcal{G}(k = 0) * e^{i\pi/2} = \mathcal{G}(k = \pi)$ , we know the eigenvalue of  $\mathcal{G}$  will be multiplied by a factor  $e^{i\pi/2}$ , when it goes from  $k = 0$  to  $k = \pi$ . Thus we know  $-i$  will evolves to 1, while  $i$  will evolves to  $-1$ . So, the pair of Kramer pair will exchange partner, when  $k$  goes from 0 to  $\pi$ .

### Weyl Semimetal

Whereas ordinary metals owe most of their unique observable character to the existence of a Fermi surface, and insulators to its lack together with the presence of a finite gap between the highest occupied and the lowest unoccupied state. The defining feature of topological semimetals is the appearance of band touching points or nodes at the Fermi energy, where two or more bands are exactly degenerate at particular values of the crystal momentum in the first Brillouin zone. Line nodes, where the bands are degenerate along closed lines in momentum space, may also exist in topological semimetals. The existence of such band touching nodes was recognized in the early days of solid-state physics<sup>21</sup>, yet their importance was only appreciated recently.

Naively, a band touching point should be a very unlikely and very unstable feature, and can thus be hardly expected to be of any importance. Indeed, as we know from basic quantum mechanics, a degeneracy between energy levels is always lifted unless required by a symmetry. However, this naive viewpoint overlooks the possibility of an accidental degeneracy of a single pair of bands in a three-dimensional material. To see how this happens, suppose two bands touch at some point,  $k_0$ , in the first BZ and at energy 0. In the vicinity of this point, the momentum-space Hamiltonian may be expanded in a Taylor series with respect to the deviation of the crystal momentum from  $k_0$ . The expansion will

generally have the form

$$H(\mathbf{K}_0 + \mathbf{q}) = \epsilon_0 \sigma_0 \pm \hbar v_F \cdot \boldsymbol{\sigma} \quad (162)$$

where  $\sigma$  are Pauli matrix. This represents nothing more than an expansion of a general  $2 \times 2$  Hermitian matrix in terms of the unit matrix and the three Pauli matrices. What makes this interesting is that there is nothing we can do to above equation to get rid of the band touching point. Changing  $\epsilon_0$  or  $k_0$  can only change the location of the band touching point in energy or crystal momentum, whereas changing the parameter  $v_F$ , which has dimensions of velocity, only changes the slope of the band dispersion away from the point. The point itself is always there. Formally, this is related to the fact that there are three crystal momentum components and the same number of Pauli matrices. This means that for such an unremovable band touching to occur we need three spatial dimensions, which is not a problem, and non-degenerate (at a general value of the crystal momentum) bands. This second requirement cannot be satisfied in a material that possesses two fundamental symmetries: inversion,  $P$  (which means that the crystal structure has an inversion centre) and time reversal,  $T$  (meaning the material is nonmagnetic). The reason is that in such a material all bands must be at least doubly degenerate at every value of  $k$  due to the fundamental property of any system of fermions that  $(PT)^2 = -1$ . Thus, we come to the conclusion that unremovable band touching points may only occur in noncentrosymmetric or magnetic materials.

Interestingly, if we set  $\epsilon_0 = 0$  in equation Eq. 162, which simply resets the energy zero-point, equation takes the exact form (up to a trivial replacement of the speed of light by  $v_F$ ) of a Weyl Hamiltonian, that is, the Hamiltonian of a massless relativistic particle of right-handed or left-handed chirality, which corresponds to the  $\pm$  sign in the equation. Due to this analogy with the Weyl equation, the touching points of pairs of non-degenerate bands are called Weyl points or nodes. Another important feature of the Weyl Hamiltonian is that it is a topologically nontrivial object. Indeed, the eigenstates of equation Eq. 162 may be labelled by helicity, which is the sign of the projection of  $\boldsymbol{\sigma}$  onto the direction of the crystal momentum  $k$ . The expectation value of  $\boldsymbol{\sigma}$  in an eigenstate of a given helicity forms a vector field in momentum space that wraps around the Weyl node location  $k_0$ , forming a hedgehog, or a hairy ball. Such a hedgehog may be characterized by a topological invariant, defined

as a flux of a vector

$$\Omega(\mathbf{q}) = \pm \frac{\mathbf{q}}{2|\mathbf{q}|^3} \quad (163)$$

through any surface in momentum space, enclosing the Weyl node, where the sign in front is the chirality of the node. This flux, normalized by  $2\pi$ , is equal to the chirality, and therefore this is a quantized integervalued invariant. The vector  $\Omega(k)$  is called the Berry curvature and the Weyl nodes may thus be regarded as point charges, which are sources and sinks of the Berry curvature. This implies that the Weyl nodes must occur in pairs of opposite chirality.

Copyright by Weizi

## TOPOLOGICAL SUPERCONDUCTOR

Topological superconductors are the non-trivial phases of superconductors described by a mean-field BdG-Hamiltonian that obey a particle-hole symmetry. excitations (Majorana modes) that are unique to topological superconductors. This symmetry allows for exotic quasi-particle In the context of topological superconductors, we will deal only with the quasiparticle physics, and we do not consider any microscopic origin of the unconventional superconductivity. In our discussion we assume that there exists some finite pairing strength, induced by interactions or occasionally through the proximity effect, and that the quasiparticle physics is well described using a mean-field formulation. Thus, we are interested in noninteracting quasiparticles that are coupled to a well-defined background pairing potential.

For comparison to more-interesting cases that are discussed later, we begin by introducing the mean-field formulation of the quasiparticle physics. We start with a simple metal with spindegeneracy given by the single-particle Hamiltonian:

$$H = \sum_{p,\sigma} \left( \frac{p^2}{2m} - \mu \right) c_{p,\sigma}^\dagger c_{p,\sigma} = \sum_{p,\sigma} E(p) c_{p,\sigma}^\dagger c_{p,\sigma}. \quad (164)$$

Formally, we can always write this Hamiltonian as

$$\begin{aligned} H &= \frac{1}{2} \left[ \sum_{p,\sigma} E(p) c_{p,\sigma}^\dagger c_{p,\sigma} - \sum_{p,\sigma} E(p) c_{p,\sigma} c_{p,\sigma}^\dagger \right] + \frac{1}{2} \sum_p E(p) \\ &= \frac{1}{2} \left[ \sum_{p,\sigma} E(p) c_{p,\sigma}^\dagger c_{p,\sigma} - \sum_{p,\sigma} E(-p) c_{-p,\sigma} c_{-p,\sigma}^\dagger \right] + \frac{1}{2} \sum_p E(p) \end{aligned} \quad (165)$$

If we introduce the spinor  $\Psi(p) = (c_{p\uparrow}, c_{p\downarrow}, c_{-p\uparrow}^\dagger, c_{-p\downarrow}^\dagger)^T$ , we can write our Hamiltonian in a more compact form:

$$H = \sum_p \Psi^\dagger(p) H_{BdG} \Psi(p), \quad H_{BdG} = \frac{1}{2} \begin{bmatrix} E(p) & 0 & 0 & 0 \\ 0 & E(p) & 0 & 0 \\ 0 & 0 & -E(-p) & 0 \\ 0 & 0 & 0 & -E(-p) \end{bmatrix} \quad (166)$$

We have introduced the subscript BdG (Bogoliubov-de-Gennes) to label the Hamiltonian written in this redundant formalism; additionally, we will drop the constant from now on. Although the statement is a bit trivial here, we note that the Bloch Hamiltonian  $H_{BdG}$  is

invariant under  $H_{BdG}(p) = CH_{BdG}^T(p)C^{-1}$ , where  $C = \tau_x \otimes I_{2 \times 2}$ . This invariance, which will become more important when we consider superconducting pairing, is known as a particle-hole or charge-conjugation “symmetry”.

The point of this formalism is to show that the easiest way to solve for the quasiparticle bands of a mean-field superconductor is to write the Hamiltonian in this BdG form. The pairing potential, which we will now introduce, simply couples the upper and lower blocks of the  $H_{BdG}$  we gave for the metal. We begin by studying the conventional s-wave, singlet pairing potential of the form  $H_\Delta = \Delta c_{p\uparrow}^\dagger c_{-p\downarrow}^\dagger + \Delta^* c_{-p\downarrow} c_{p\uparrow}$ . This term, at the mean-field level, leads to a nonconservation of charge, i.e., charge is conserved only modulo  $2e$ . This term captures the physics of two electrons or holes combining to form a Cooper pair or a Cooper pair breaking apart into its constituents.

Next we use an example of a chiral p-wave superconductor.

$$H_{BdG} = \left(\frac{p^2}{2m} - \mu\right)\tau_z + \Delta_0(p_x\tau_x - p_y\tau_y). \quad (167)$$

The Pauli matrices  $\tau_{x,y,z}$  act on the particle-hole degree of freedom. The normal part is a parabolic dispersion with momentum  $p$ , effective mass  $m$  and chemical potential  $\mu$ . The pair potential  $\Delta_0$  pairs electrons of opposite momenta, but equal spin. The Hamiltonian anti-commutes with the particle-hole symmetry operator  $P = \tau_x K$ , which squares to 1 and places the chiral p-wave superconductor in symmetry class D of the tenfold way. More general Hamiltonians in this symmetry class have the form  $H(p) = h_x(p)\tau_x + h_y(k)\tau_y + h_z(k)\tau_z$ . Particle-hole symmetry excludes a term  $\tau_0$  and requires  $h_{x,y}(p) = -h_{x,y}(-p)$ ,  $h_z(-k) = h_z(k)$ . We can define the normalized Bloch vector  $\mathbf{h}(k) = \mathbf{h}(k)/|\mathbf{h}(k)|$ , where  $\mathbf{h} = (h_x, h_y, h_z)$ . The Z-topological invariant  $n$  is the Chern number  $n = \frac{1}{4\pi} \oint dk_x dk_y (\partial_{k_x} \mathbf{h} \times \partial_{k_y} \mathbf{h}) \cdot \mathbf{h}$ .

### Majorana edge modes

The simplest possible case where we expect to see such topological edge modes is a domain wall  $\mu = -\mu_0$  for  $y < 0$  and  $\mu = \mu_0$  for  $y > 0$ . All eigenstates of the Bogoliubov-De Gennes equation are then plane waves in the x-direction. To find the edge modes, we need to solve the corresponding eigenvalue problem in real space

$$\begin{pmatrix} -\mu(y) & -\Delta_0(\partial_y - k_x) \\ -i\Delta_0(\partial_y + k_x) & \mu(y) \end{pmatrix} \begin{pmatrix} \phi_e(y) \\ \phi_h(y) \end{pmatrix} = E \begin{pmatrix} \phi_e(y) \\ \phi_h(y) \end{pmatrix} \quad (168)$$

where  $\Psi(r, t) = \begin{pmatrix} \phi_e(y) \\ \phi_h(y) \end{pmatrix} e^{ik_x x - Et}$ .

The solution is  $E = \mp \Delta_0 k_x$ ,

$$\Psi \sim \begin{pmatrix} e^{\mp i\pi/4} \\ e^{\pm i\pi/4} \end{pmatrix} e^{\pm \frac{\mu_0}{\Delta_0} |y|} e^{ik_x x - Et} \quad (169)$$

Copyright by Weizl

## THE KITAEV CHAIN

Let's start from the creation and annihilation operators  $c^\dagger$  and  $c$  of a fermionic mode. These operators satisfy the anticommutation relation  $\{c^\dagger, c\} = 1$  and, furthermore, square to zero,  $c^2 = 0$  and  $(c^\dagger)^2 = 0$ . They connect two states  $|0\rangle$  and  $|1\rangle$ , which correspond to the 'vacuum' state with no particle and the 'excited' state with one particle, according to the following rules  $c|0\rangle = 0$ ,  $c^\dagger|0\rangle = |1\rangle$ , and  $c|1\rangle = |0\rangle$ .

You can write them down in the following way

$$c^\dagger = \frac{1}{2}(\gamma_1 + i\gamma_2), c = \frac{1}{2}(\gamma_1 - i\gamma_2) \quad (170)$$

The operators  $\gamma_1$  and  $\gamma_2$  are known as Majorana operators. By inverting the transformation above, you can see that  $\gamma_1^\dagger = \gamma_1, \gamma_2^\dagger = \gamma_2$ . Because of this property, we cannot think of a single Majorana mode as being 'empty' or 'filled', as we can do for a normal fermionic mode. This makes Majorana modes special. They satisfy the commutator:

$$\{\gamma_j^\dagger, \gamma_i\} = 2\delta_{ij}, \{\gamma_i, \gamma_j\} = 2\delta_{ij} \quad (171)$$

Let us now try to write the Hamiltonian.

$$H = -\mu \sum_n c_n^\dagger c_n - t \sum_n [c_n^\dagger c_{n+1} + h.c.] + \Delta \sum_n [c_n c_{n+1} + h.c.] \quad (172)$$

With a homogenous  $|\Delta|$ , we have

$$H_{BdG} = \sum_p \Psi_p^\dagger H(p) \Psi(p) = \frac{1}{2} \sum_p (c_p, c_{-p}^\dagger) \begin{pmatrix} -2t \cos p - \mu & 2i|\Delta| \sin p \\ -2i|\Delta| \sin p & 2t \cos p + \mu \end{pmatrix} \quad (173)$$

The energy spectrum is  $E_\pm = \pm \sqrt{(2t \cos p + \mu)^2 + 4|\Delta|^2 \sin^2 p}$ .

The BdG Hamiltonian has the particle-hole symmetry.  $PH_{BdG}P^{-1} = -H_{BdG}$ , or  $H(p) = -\tau_x H^*(-k) \tau_x$ . Given a solution with energy  $E$  and momentum  $p$ , particle-hole symmetry dictates in general the presence of a solution with energy  $-E$  and momentum  $-p$ .

We focus on the gap closing at  $\mu = -2t$ , which happens at  $p = 0$ . Close to this point where the two bands touch, we can make a linear expansion of the Hamiltonian,

$$H(p) = m\tau_z + 2\Delta p\tau_y \quad (174)$$

with  $m = -\mu - 2t$ . We see the effective Hamiltonian is a Dirac Hamiltonian. The "mass"  $m$  appearing in this Dirac Hamiltonian is a very important parameter to describe what

is happening. Its sign reminds us of the two different phases.  $m < 0$  for  $\mu > -2t$ , which corresponds to the topological phase, the one with Majorana modes in the open chain;  $m > 0$  for  $\mu < -2t$ , which corresponds to the trivial phase, the one without Majorana modes in the open chain (see SSH model). In topological phase, the edge mode relates to zero energy state. Recall that we are dealing with a particle-hole symmetric Hamiltonian. Hence, the spectrum has to be symmetric around zero energy. Trying to move these levels from zero energy individually is impossible, as it would violate particle-hole symmetry.

This physics is more transparent, when we write it use Majorana picture:

$$H_{BdG} = \frac{i}{2} \sum_j (-\mu \gamma_{1,j} \gamma_{2,j} + (t + |\Delta|) \gamma_{2,j} \gamma_{1,j+1} + (-t + |\Delta| \gamma_{1,j} \gamma_{2,j+1})) \quad (175)$$

Copyright by Weizhi



class	$\mathcal{C}$	$\mathcal{P}$	$\mathcal{T}$	$d = 0$	1	2	3	4	5	6	7
A				$\mathbb{Z}$		$\mathbb{Z}$		$\mathbb{Z}$		$\mathbb{Z}$	
AIII	1				$\mathbb{Z}$		$\mathbb{Z}$		$\mathbb{Z}$		$\mathbb{Z}$
AI			1	$\mathbb{Z}$				$2\mathbb{Z}$		$\mathbb{Z}_2$	$\mathbb{Z}_2$
BDI	1	1	1	$\mathbb{Z}_2$	$\mathbb{Z}$				$2\mathbb{Z}$		$\mathbb{Z}_2$
D		1		$\mathbb{Z}_2$	$\mathbb{Z}_2$	$\mathbb{Z}$				$2\mathbb{Z}$	
DIII	1	1	-1		$\mathbb{Z}_2$	$\mathbb{Z}_2$	$\mathbb{Z}$				$2\mathbb{Z}$
AII			-1	$2\mathbb{Z}$		$\mathbb{Z}_2$	$\mathbb{Z}_2$	$\mathbb{Z}$			
CII	1	-1	-1		$2\mathbb{Z}$		$\mathbb{Z}_2$	$\mathbb{Z}_2$	$\mathbb{Z}$		
C		-1				$2\mathbb{Z}$		$\mathbb{Z}_2$	$\mathbb{Z}_2$	$\mathbb{Z}$	
CI	1	-1	1				$2\mathbb{Z}$		$\mathbb{Z}_2$	$\mathbb{Z}_2$	$\mathbb{Z}$

FIG. 14: Periodic Table.

### AT A GLANCE: PERIODIC TABLE

The possible symmetry classes in various dimensions gives what kind of topological insulators are possible.

An empty entry means that the system does not have a topological phase. In other words, all gapped Hamiltonians with dimension and symmetries corresponding to an empty entry can be deformed into each other, without ever closing the bulk gap and without breaking any existing symmetry.

A  $\mathbb{Z}$  entry tells us that the topological invariant is an integer number,  $Q = 0, \pm 1, \pm 2, \dots$ . An example of such a system is the quantum Hall effect, for which the topological invariant is the Chern number. The value of chern number specifies the number of chiral edge states and their chirality.

A  $2\mathbb{Z}$  entry is much like a  $\mathbb{Z}$  entry, except that the invariant may only take even numbers,  $Q = 0, \pm 2, \dots$ , because of some doubling of the degrees of freedom. An example is a quantum dot with spinful time-reversal symmetry, for which the topological invariant is the number of filled energy levels. It may only be an even number because of Kramers degeneracy.

A  $\mathbb{Z}_2$  entry means that there are only two distinct topological phases, with  $Q = \pm 1$  or  $Q = 0, 1$ . An example we know is the Majorana chain, with the Pfaffian topological invariant, which distinguishes between the two phases with or without unpaired Majorana modes and the ends. Another example we know are the time-reversal invariant topological insulators in two and three dimensions.

Each row in the table corresponds to a certain symmetry class, that is to a given com-

combination of the presence or absence of three fundamental discrete symmetries. They are time-reversal symmetry (T), particle-hole symmetry (P) and chiral symmetry (C). The chiral symmetry C is as sublattice symmetry. This is because in condensed matter physics, a natural realization of chiral symmetry is a system composed of two sublattices, such that sites in one lattice only couple to sites in the other.

Why do we consider these symmetries fundamental, and restrict the periodic table to them only? Time-reversal, particle-hole and chiral symmetries act in a special way. They impose certain constraints on an irreducible Hamiltonian - for instance, by forcing it to be a real matrix, or to be block off-diagonal.

T is an anti-unitary operator which commutes with the Hamiltonian. P is an anti-unitary operator which anti-commutes with the Hamiltonian. C is a unitary operator which anti-commutes with the Hamiltonian.

Thus, a system can behave in three ways under time-reversal symmetry T: (1) it does not have time-reversal symmetry, (2) it has it and  $T^2 = 1$ , (3) it has it and  $T^2 = -1$ . The same holds for particle-hole symmetry, which can also have  $P^2 = \pm 1$ . On the other hand, the chiral symmetry only comes in one flavor,  $C^2 = 1$ . The important thing to notice now is that C is not completely independent from T and P. Whenever a system has both T and P, there is also a chiral symmetry  $C=PT$ . Adding all the possibilities, we indeed find 10 symmetry classes, as shown in the Tab.

---

\* Electronic address: zhuwei@westlake.edu.cn

- [1] E. Fradkin, Field Theories of Condensed Matter Physics. Cambridge University Press, 2013.
- [2] A. Bernevig and Talyor, Topological insulators.

Copyright by Wei Zi.